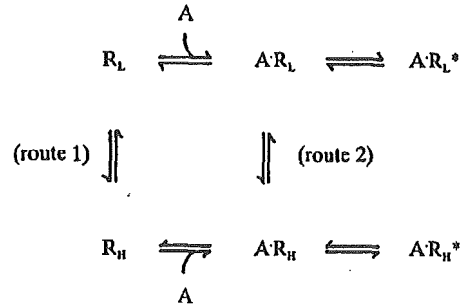

Scheme 4.

may be involved. We propose the following modification to Scheme 2.

This model (Scheme 4) involves two voltage-dependent processes, one resulting in activation through "route 1", and the other resulting in deactivation through "route 2". Such model would explain the observed difference in voltage dependence between activation and deactivation. However, we would expect this model to result in more difficult to interpret data than we did above based on Schemes 2 and 3.

4.2. Relevance of voltage-dependent gating

$P2X_2$ receptor is expressed in a number of neurons (e.g., Atkinson et al., 2000; Rubio and Soto, 2001). $P2X_2$ receptor/channel is permeable to Ca^{2+} (Egan and Khakh, 2004), and Ca^{2+} influx through the channel may influence cellular activity, although its exact role remains to be clarified. The voltage-dependent gating reported here may be relevant to the Ca^{2+} influx from the following consideration. Na^+ current (I_{Na}) and Ca^{2+} current (I_{Ca}) permeating through $P2X_2$ receptor/channel are:

$$I_{Na} = -P_{Na}\frac{E_m F^2}{RT}\frac{[Na]_o}{1-\exp(-EF/RT)} \quad (3)$$

$$I_{Ca} = -4P_{Ca}\frac{E_m F^2}{RT}\frac{[Ca]_o \exp(-2EF/RT)}{1-\exp(-2EF/RT)}, \quad (4)$$

where P_{Na} and P_{Ca} represent the permeability of Na^+ and Ca^{2+}, respectively, E_m represents the membrane potential, and F, R, and T are their usual physicochemical meanings (Fatt and Ginsborg, 1958; Nakazawa et al., 1989). The ratio of I_{Na} to I_{Ca} is thus:

$$\frac{I_{Ca}}{I_{Na}} = \frac{4P_{Ca}[Ca]_o}{P_{Na}[Na]_o}\frac{1}{\exp(E_m F/RT)[\exp(E_m F/RT)+1]} \quad (5)$$

This equation indicates that the ratio of I_{Ca}/I_{Na} is larger at more negative potentials. The ratio calculated at −90 mV is about 13-fold larger than that calculated at −30 mV. Thus, channel opening at negative potentials favors Ca^{2+} over Na^+ influx. Thus, voltage-dependent gating may facilitate cellular Ca^{2+}-dependent responses when cells are hyperpolarized. This may occur when efflux through K^+ channels outpaces depolarization afforded by opening of $P2X_2$ receptor/channels.

4.3. Conclusion

The results of the present study suggested that $P2X_2$ receptor exhibits voltage-dependent gating, and that this is not due to simple activation and deactivation of a single gate, but rather, due to a transition from a low ATP affinity to a high ATP affinity state. This may favor Ca^{2+} influx at negative potentials, although further studies are required to clarify the physiological significance of voltage-dependent gating of $P2X_2$ receptor.

Acknowledgements

This work was supported, in part, by a Health and Labour Science Research Grant for Research on Advanced Medical Technology from the Ministry of Health, Labour and Welfare, Japan, as well as a grant-in-aid for scientific research from the Ministry of Education, Science, Sports and Culture, Japan (KAKENHI 13672319) awarded to K.N.

References

Atkinson, L., Batten, T.F., Deuchars, J., 2000. $P2X_2$ receptor immunoreactivity in the dorsal vagal complex and area postrema of the rat. Neuroscience 99, 683–696.

Brake, A.J., Wagenbach, M.J., Julius, D., 1994. New structural motif for ligand-gated ion channels defined by an ionotropic ATP receptor. Nature 371, 519–523.

Clyne, J.D., LaPointe, L.D., Hume, R.I., 2002. The role of histidine residues in modulation of the rat $P2X_2$ purinoceptor by zinc and pH. J. Physiol. 539, 347–359.

Egan, T., Khakh, B.S., 2004. Contribution of calcium ions to P2X channel responses. J. Neurosci. 24, 3413–3420.

Egan, T.M., Haines, W.R., Voigt, M.M., 1998. A domain contributing to the ion channel of ATP-gated $P2X_2$ receptors identified by the substituted cysteine accessibility method. J. Neurosci. 18, 2350–2359.

Ennion, S., Hagan, S., Evans, R.J., 2000. The role of positively charged amino acids in ATP recognition by human $P2X_1$ receptors. J. Biol. Chem. 275, 29361–29367.

Fatt, P., Ginsborg, B.L., 1958. The ionic requirements for the production of action potentials in crustacean muscle fibres. J. Physiol. 142, 516–543.

Haines, W.R., Migita, K., Cox, J.A., Egan, T.M., Voigt, M.M., 2001. The first transmembrane domain of the P2X receptor subunit participates in the agonist-induced gating of the channel. J. Biol. Chem. 276, 32793–32798.

Hille, B., 1992a. Classical biophysics of the squid giant axon. Ionic channels of excitable membranes, Second Edition. Sinauer, Sunderland, MA, pp. 23–58.

Hille, B., 1992b. Ligand-gated channels of fast chemical synapses. Ionic channels of excitable membranes, Second Edition. Sinauer, Sunderland, MA, pp. 140–169.

Hodgkin, A.L., Huxley, A.F., 1952. The dual effect of membrane potential on sodium conductance in the giant axon of *Loligo*. J. Physiol. 116, 497–506.

Jiang, L.H., Rassendren, F., Surprenant, A., North, R.A., 2000. Identification of amino acid residues contributing to the ATP-binding site of a purinergic P2X receptor. J. Biol. Chem. 275, 34190–34196.

Jiang, L.H., Rassendren, F., Spelta, V., Surprenant, A., North, R.A., 2001. Amino acid residues involved in gating identified in the first membrane-spanning domain of the rat $P2X_2$ receptor. J. Biol. Chem. 276, 14902–14908.

Khakh, B.S., 2001. Molecular physiology of P2X receptors and ATP signalling at synapses. Nat. Rev. 2, 165–174.

Migita, K., Haines, W.R., Voigt, M.M., Egan, T.M., 2001. Polar residues of the second transmembrane domain influence cation permeability of the ATP-gated $P2X_2$ receptor. J. Biol. Chem. 276, 30934–30941.

Nakazawa, K., Ohno, Y., 1997. Effects of neuroamines and divalent cations on cloned and mutated ATP-gated channels. Eur. J. Pharmacol. 325, 101–108.

Nakazawa, K., Fujimori, K., Takanaka, A., Inoue, K., 1989. An ATP-activated conductance in pheochromocytoma cells and its suppression by extracellular calcium. J. Physiol. 428, 257–272.

Nakazawa, K., Liu, M., Inoue, K., Ohno, Y., 1997a. pH dependence of facilitation by neurotransmitters and divalent cations of $P2X_2$ purinoceptor/channels. Eur. J. Pharmacol. 337, 309–314.

Nakazawa, K., Liu, M., Inoue, K., Ohno, Y., 1997b. Voltage-dependent gating of ATP-activated channels in PC12 cells. J. Neurophysiol. 78, 884–890.

Nakazawa, K., Ojima, H., Ohno, Y., 2002. A highly conserved tryptophane residue indispensable for cloned rat neuronal P2X receptor activation. Neurosci. Lett. 324, 141–144.

North, R.A., 2002. Molecular physiology of P2X receptors. Physiol. Rev. 82, 1013–1067.

North, R.A., Surprenant, A., 2000. Pharmacology of cloned P2X receptors. Annu. Rev. Pharmacol. Toxicol. 40, 563–580.

Ralevic, V., Burnstock, G., 1998. Receptors for purines and pyrimidines. Pharmacol. Rev. 50, 413–492.

Rassendren, F., Buell, G., Newbolt, A., North, R.A., Surprenant, A., 1997. Identification of amino acid residues contributing to the pore of a P2X receptor. EMBO J. 16, 3446–3454.

Roberts, J.A., Evans, R.J., 2004. ATP binding at human $P2X_1$ receptors. Contribution of aromatic and basic amino acids revealed using mutagenesis and partial agonists. J. Biol. Chem. 279, 9043–9055.

Rubio, M., Soto, F., 2001. Distinct localization of P2X receptors at excitatory postsynaptic specializations. J. Neurosci. 21, 641–653.

Weber, W.-M., 1999. Ion currents of *Xenopus laevis* oocytes: state of the art. Biochim. Biophys. Acta 1421, 213–233.

Zhang, Y., Hamill, O.P., 2000. Calcium, voltage- and osmotic stress sensitive currents in *Xenopus* oocytes and their relationship to single mechanically gated channels. J. Physiol. 523, 83–99.

Available online at www.sciencedirect.com
SCIENCE DIRECT
European Journal of Pharmacology 518 (2005) 107 – 110
www.elsevier.com/locate/ejphar

Short communication

Purification and aqueous phase atomic force microscopic observation of recombinant $P2X_2$ receptor

Ken Nakazawa [a,*], Yoko Yamakoshi [b,1], Toshie Tsuchiya [c], Yasuo Ohno [a]

[a] *Division of Pharmacology, National Institute of Health Sciences, 1-18-1 Kamiyoga, Setagaya, Tokyo 158-8501, Japan*
[b] *Division of Organic Chemistry, National Institute of Health Sciences, 1-18-1 Kamiyoga, Setagaya, Tokyo 158-8501, Japan*
[c] *Division of Medical Devices, National Institute of Health Sciences, 1-18-1 Kamiyoga, Setagaya, Tokyo 158-8501, Japan*

Received 4 April 2005; received in revised form 14 June 2005; accepted 20 June 2005
Available online 28 July 2005

Abstract

Recombinant $P2X_2$ receptor was observed by atomic force microscope in the aqueous phase. The $P2X_2$ receptor was expressed in an insect cell line, and recombinant proteins were prepared under native conditions. The membrane fractions were extracted, and histidine-tagged receptor protein was purified from the fractions by column chromatography. When the purified protein fraction was diluted with water and served for atomic force microscopy, dispersed particles of about 3 nm in height were observed. In the presence of 1 mM ATP, the assembly-like images of the particles were obtained. More densely assembled images of the particles were achieved when the protein was dissolved in a Tris buffer containing 1 mM ATP. Under this condition, imaging of the surface of the particles exhibited a circular structure with a diameter of about 10 nm having a pore-like structure. These results suggest that atomic force microscopy provides structural information about $P2X_2$ receptor in aqueous phase.

Keywords: P2X receptor; Atomic force microscopy; Protein structure; ATP

1. Introduction

P2X receptors are ion channel forming membrane proteins that are activated by extracellular ATP, and their physiological roles have been shown in various tissues including the central nervous system (see reviews, Khakh, 2001; North, 2002; Vial et al., 2004). This ion channel/receptor family consists of 7 subclasses ($P2X_1$ to $P2X_7$), and is believed to have molecular structures distinct from so-called "ligand-gated channel super family" including nicotinic acetylcholine receptor/channels and ionotropic glutamate receptor channels. Structural analyses such as the X-ray crystal analysis have not been made for P2X receptor/channel family. In addition, because of their distinct structures, estimation from homology modeling based on known three-dimensional structures of other proteins is difficult. Thus, information concerning the structure and morphology of P2X receptor is lacking. Atomic force microscopy is an approach for structural analysis that allows the analysis of a small amount (nanogram to microgram) of uncrystalized protein. Atomic microscopy enables the observation of both individual and assembled protein molecules in the aqueous phase, which may reveal dynamic forms of biologically active proteins (Müller and Engel, 2002). Recently, Barrera et al. (2005) reported atomic force microscopy imaging of dried P2X receptor protein. In the present study, we have prepared $P2X_2$ receptor protein from an insect cell line expression system, and made atomic force microscopy imaging in aqueous phase. The imaging has revealed that $P2X_2$ receptor is a pore-forming protein for the first time.

* Corresponding author. Tel.: +81 3 3700 9704; fax: +81 3 3707 6950.
E-mail address: nakazawa@nihs.go.jp (K. Nakazawa).
[1] Present address: Center for Polymers and Organic Solids, Department of Chemistry and Biochemistry, University of California, Santa Barbara, CA 93106-9510, USA.

0014-2999/$ - see front matter © 2005 Elsevier B.V. All rights reserved.
doi:10.1016/j.ejphar.2005.06.018

2. Materials and methods

2.1. Preparation of recombinant $P2X_2$ receptor protein

N-terminal hexahistidine-tagged recombinant rat $P2X_2$ receptor was expressed using baculovirus-Sf9 system, which has been used for the expression of membrane receptor proteins (e.g., Boundy et al., 1993; Ng et al., 1993). cDNA encoding rat $P2X_2$ receptor (Brake et al., 1994) was subcloned into pFast BAC HTc vector (BD Bioscience Clonetech, Palo Alto, CA, USA). The recombinant virus was transfected to insect-derived clonal Sf9 cells. After culturing at a volume of 500 ml at room temperature, the culture medium was centrifuged at 130 $\times g$ for 5 min, and the precipitated cells were washed with Ca^{2+}, Mg^{2+}-free phosphate buffered saline (137 mM NaCl, 2.7 mM KCl, 8.1 mM Na_2HPO_4, and 1.5 mM KH_2PO_4; PBS(−)) twice. The cells were then suspended in a Tris–HCl (pH 7.4) lysis buffer containing Triton X-100, and homogenized. NaCl was added such that its final concentration became 100 mM. This solution was centrifuged at 30000 $\times g$ for 20 min, and the supernatant was then centrifuged at 380000 $\times g$ for 10 min. Polyacrylamide gel electrophoresis followed by immunoblotting analysis with anti-hexahistidine antibody showed that hexahistidine-tagged proteins of an expected size (56 kD) were found in this supernatant. Further purification was made using Chelating Sepharose FF colums. Ni^{2+}-bound columns were equilibrated with a buffer containing 20 mM Tris–HCl and 0.5 M NaCl (pH 8.0), and samples were applied. The bound receptor proteins were eluted by stepwise increase of imidazole (10, 20, 50, 100, 200 and 500 mM). The concentrations of the receptor protein in the eluted solutions were estimated by measuring absorbance at 595 nm. The most purified $P2X_2$ receptor protein (>90% of total protein) was found in the fraction eluted by 10 mM imidazole, and this fraction was served for atomic force microscopy imaging. The purified $P2X_2$ receptor exhibited the ability to bind ATP when photoaffinity labeling with [α-^{32}P]ATP was performed according to Kim et al. (1997). In this experiment, the binding of [α-^{32}P]ATP was markedly reduced by 100 μM nonradiolabeled ATP.

2.2. Atomic force microscopy imaging

The protein solution (about 1.5 μM) was diluted to appropriate concentrations (0.1 to 10 nM) with water, and the diluted solution was placed on freshly cleaved mica. After 30 min, unbound proteins were washed away with water, and served for atomic force microscopy imaging. When ATP (disodium salt; Sigma, St. Louis, MO, USA) was added to water, 1 mM solution was neutralized to pH 7.4 with 2 N NaOH (final Na^+ concentration was about 16 mM). In part of the experiments, the protein solution was diluted with a Tris buffer of the following composition (in millimolar): Tris 50, KCl 150, $MgCl_2$ 10, dithiothreirol 1 (pH 7.0). This buffer composition was similar to that utilized for atomic force microscopy imaging of *Escherichia coli* GroES (Cheung et al., 2000). Imaging was made in an aqueous tapping mode using MFP-3D (Asylum Research, Santa Barbara, CA, USA) equipped with OMCL-TR800PSA (Olympus, Tokyo, Japan) as a probe.

3. Results

Fig. 1A shows atomic force microscopy images of purified $P2X_2$ receptor proteins in water. A larger part of the proteins were found as dispersed particles. The height of single $P2X_2$ receptor proteins was about 3 nm (Fig. 1B). In the presence of 1 mM ATP, larger particles, presumably clots of several receptor proteins, were observed in addition to dispersed particles (Fig. 1C). A flatly and densely assembled image was obtained when the proteins were dissolved in a Tris buffer containing 1 mM ATP (Fig. 2A). Densely packed assembly is advantageous for atomic force microscopy imaging because resolution is improved due to smaller movement of probes along Z-axis (Müller and Engel, 2002). When the protein assembly shown in Fig. 2A was imaged at higher magnification, a circular structure with a pore was observed (Fig. 2B). The diameter of the circular structure was about 10 nm, and that of the pore was several nanometers. Without ATP, the protein was not densely assembled and did not exhibit uniform direction (not shown).

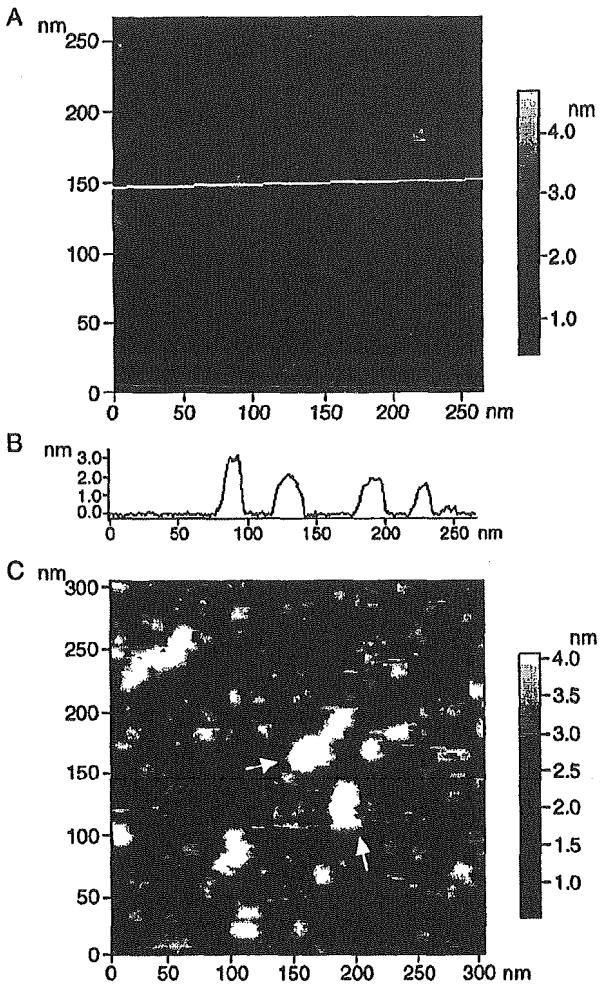

Fig. 1. (A) An atomic force microscopy image of $P2X_2$ receptor proteins in water. Isolated single receptor proteins and their small assemblies are seen. (B) A section of the image shown in (A). The section was made along with the line. The height of receptor proteins is about 3 nm or less. (C) An image of $P2X_2$ receptor proteins in the presence of 1 mM ATP. In addition to single receptor proteins, clots of the proteins (indicated by arrows) were also seen.

4. Discussion

For atomic force microscopy imaging of membrane proteins, densely expressed proteins in particular cells have

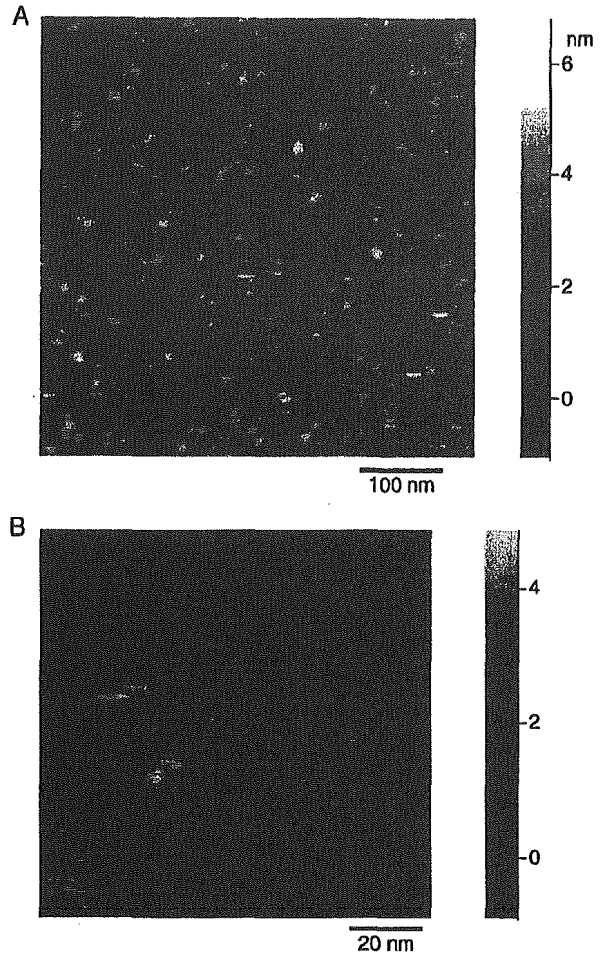

Fig. 2. (A) An image of $P2X_2$ receptor proteins in a Tris buffer containing 1 mM ATP. The proteins were flatly and densely assembled. (B) An expanded image. The upper surfaces of individual proteins exhibited a circular structure having a pore in its center.

been served in the presence of lipid bilayers (Müller and Engel, 2002; Müller et al., 2002). This two-dimensional (2D) protein crystal can provide high resolution of images, especially when combined with image processing including averaging. However, preparation of 2D crystals requires skilled techniques or special equipment. The present study has shown that recombinant $P2X_2$ can be imaged by atomic force microscopy without special techniques, but by simply adding agonist molecule, ATP. The role of ATP in promoting the densely packed assembly is unclear at present. It is speculated that receptor protein molecules without ATP freely move and exhibit various conformations, whereas ATP-bound receptor molecules exhibit only one or a restricted number of conformations in aqueous phase. The pore identified in the center of the protein may be the ion channel involved in $P2X_2$ receptor. A similar pore has been observed in connexin that also forms ion channels (Müller et al., 2002). It is unclear that the pore corresponds to the inner mouth or the outer mouth of the channel. Nevertheless, it is interesting that a number of proteins appear to exhibit similar surface structure (Fig. 2B). P2X receptor possesses a large extracellular domain, and, thus, it is possible that this domain is orientated upward to increase contact with the aqueous phase. Atomic force microscopy imaging of isolated membrane proteins may be less advantageous to elucidate biological functions compared to those embedded in lipid bilayer. However, isolated proteins are more readily observed than membrane preparations, and the imaging of these proteins may provide insights into the intrinsic properties of proteins and useful information to clarify the interactions between proteins and the membrane.

Barrera et al. (2005) observed dried $P2X_2$ receptor protein as a simple particle. We have revealed the outer structure of the protein, suggesting that resolution was better in the present study. However, our observation has not resolved trimeric assembly of $P2X_2$ receptor protein, which has been shown using antibodies specific for the protein (Barrera et al., 2005). Trimeric assembly of P2X receptor has been also demonstrated by electrophysiological and biochemical studies, and two transmembrane regions of each subunit are believed to contribute to the forming of channel pore (North, 2002; Vial et al., 2004). If $P2X_2$ receptor forms a six-barrel channel like connexin, this may account for a similar pore size (about several nanometers). Further improvement will be necessary to identify individual subunit proteins that form $P2X_2$ receptor and clarify more detailed structure by atomic force microscopy.

Acknowledgments

We are grateful to Dr. Jeffrey W. Bode of Department of Chemistry and Biochemistry, University of California, Santa Barbara for improving our manuscript. This work was partly supported by a Health and Labour Science Research Grant for Research on Advanced Medical Technology from the Ministry of Health, Labour and Welfare, Japan awarded to K.N., Y.Y. and T.T., and a grant-in-aid for scientific research from the Ministry of Education, Science, Sports and Culture, Japan (KAKENHI 13672319) awarded to K.N.

References

Barrera, N.P., Ormond, S.J., Henderson, R.M., Murrell-Langnado, R.D., Edwardson, J.M., 2005. AFM imaging demonstrates that $P2X_2$ receptors are trimers, but that $P2X_6$ receptor subunits do not oligomerize. J. Biol. Chem. 280, 10759–10765.

Boundy, V.A., Luedtke, R.R., Gallitano, A.L., Smith, J.E., Filtz, T.M., Kallen, R.G., Molinoff, P.B., 1993. Expression and characterization of the rat D3 dopamine receptor: properties and development of antibodies. J. Pharmacol. Exp. Ther. 264, 1002–1011.

Brake, A.J., Wagenbach, M.J., Julius, D., 1994. New structural motif for ligand-gated ion channels defined by an ionotropic ATP receptor. Nature 371, 519–523.

Cheung, C.L., Hafner, J.H., Lieber, C.M., 2000. Carbone nanotube atomic force microscopy tips: direct growth by chemical vapor deposition and application to high-resolution imaging. Proc. Natl. Acad. Sci., U. S. A. 97, 3809–3813.

Khakh, B.S., 2001. Molecular physiology of P2X receptors and ATP signalling at synapses. Nat. Rev. 2, 165–174.

Kim, M., Yoo, O.J., Choe, S., 1997. Molecular assembly of the extracellular domain of $P2X_2$, an ATP-gated ion channel. Biochem. Biophys. Res. Commun. 240, 618–622.

Müller, D.J., Engel, A., 2002. Conformations, flexibility, and interactions observed on individual membrane proteins by atomic force microscopy. Methods Cell Biol. 68, 257–298.

Müller, D.J., Hand, G.M., Engel, A., Soslinsky, G., 2002. Conformational changes in surface structures of isolated connexin 26 gap junctions. EMBO J. 21, 3598–3607.

Ng, G.Y., George, S.R., Zastawny, R.L., Caron, M., Bouvier, M., Dennis, M., O'Dowd, B.F., 1993. Human serotonin 1B receptor expression in Sf9 cells: phosphorylation, palmitoylation, and adenylyl cyclase inhibition. Biochemistry 32, 11727–11733.

North, R.A., 2002. Molecular physiology of P2X receptors. Physiol. Rev. 82, 1013–1067.

Vial, C., Roberts, J.A., Evans, R.J., 2004. Molecular properties of ATP-gated P2X receptor ion channels. Trends Pharmacol. Sci. 25, 487–493.

Environmental and Molecular Mutagenesis 45:162–176 (2005)

Review Article

Generation of Loss of Heterozygosity and Its Dependency on p53 Status in Human Lymphoblastoid Cells

Masamitsu Honma*

Division of Genetics and Mutagenesis, National Institute of Health Sciences, Tokyo, Japan

Loss of heterozygosity (LOH) is a critical event in the development of human cancers. LOH is thought to result from either a large deletion or recombination between homologous alleles during repair of DNA double-strand breaks (DSBs). These types of genetic alterations produce mutations in the *TK* gene mutation assay, which detects a wide mutational spectrum, ranging from point mutations to LOH-type mutations. TK6, a human lymphoblastoid cell line, is heterozygous for the thymidine kinase (*TK*) gene and has a wild-type *p53* gene. The related cell lines, TK6-E6 and WTK-1, which are p53-deficient and p53-mutant (Ile237), respectively, are also heterozygous for the *TK* gene and LOH-type mutation can be detected in these cells. Therefore, comparative studies of *TK* mutation frequency and spectrum with these cell lines are useful for elucidating the role of p53 in generating LOH and maintaining genomic stability in human cells. We demonstrate here that LOH and its associated genomic instability strongly depend on the p53 status in these cells. TK6-E6 and WTK-1 are defective in the G1/S checkpoint and in apoptosis. Unrepaired DSBs that escape from the checkpoint can potentially initiate genomic instability after DNA replication, resulting in LOH and a variety of chromosome changes. Moreover, genomic instability is enhanced in WTK-1 cells. It is likely that the mutant p53 protein in WTK-1 cells increases LOH in a dominant-negative manner due to its abnormal recombination capacity. We discuss the mutator phenotype and genomic instability associated with p53 inactivation with the goal of elucidating the mechanisms of mutation and DNA repair in untargeted mutagenesis. Environ. Mol. Mutagen. 45:162–176, 2005. © 2005 Wiley-Liss, Inc.

Key words: loss of heterozygosity; p53; DNA double-strand breaks; DNA repair; recombination; genomic stability

INTRODUCTION

Cancer is a genetic disease of somatic cells. Alteration of DNA is a fundamental event that allows a normal somatic cell to transform into a tumor cell. Various kinds of genetic damage are observed in tumor cells, including point mutation, deletion, translocation, gene amplification, and aneuploidy. The genetic changes affecting the function or expression of oncogenes or tumor suppressor genes accumulate during tumor development, ultimately producing the neoplastic phenotype. Proto-oncogene products normally stimulate cell proliferation, while tumor suppressor genes seem to function in cell growth control by regulating the cell cycle or by mediating cellular responses to DNA damage.

A single mutation in a proto-oncogene is sufficient to endow oncogenic activity and cell conversion to a premalignant phenotype. Mutations in tumor suppressor genes are, on the other hand, generally recessive. In the classical two-hit theory, a mutation in one allele of a tumor suppressor gene does not disrupt growth control as long as the second allele is functional [Lasko et al., 1991]. To result in a mutant phenotype, mutations must sequentially occur in both alleles of the gene. Typically, a point mutation first occurs in one allele, followed by loss of the remaining wild-type allele, although several combinations are possible. Allele loss can be recognized as loss of heterozygosity (LOH) by analyzing polymorphic DNA markers within or near the tumor suppressor gene [Lasko et al., 1991]. Since the inactivation of tumor suppressor

Grant sponsor: the Nuclear Energy Research Grants from the Ministry of Education, Culture, Sports, Science, and Technology of Japan.

*Correspondence to: Masamitsu Honma, Division of Genetics and Mutagenesis, National Institute of Health Sciences, 1-18-1 Kamiyoga, Setagaya-ku, Tokyo 158-8501, Japan. E-mail: honma@nihs.go.jp

Invited article: 25th anniversary of *Environmental and Molecular Mutagenesis*

DOI 10.1002/em.20113

Published online 1 February 2005 in Wiley InterScience (www.interscience.wiley.com).

genes rather than the activation of proto-oncogenes is frequently associated with human sporadic and heritable cancers, LOH is considered an important event in human tumorigenesis [Kinzler and Vogelstein, 1996].

LOH was first observed in retinoblastoma [Cavenee et al., 1983], with LOH detected in the *RB1* gene on chromosome 13q in approximately 70% of both heritable and sporadic retinoblastoma [Cavenee et al., 1985]. Also, LOH of the *BRCA1* gene has been detected in more than 80% of breast and ovarian cancers [Neuhausen and Marshall, 1994] and LOH of the *VHL* gene in more than 90% of von Hippel Lindau renal tumors [Gnarra et al., 1994]. Furthermore, mutations of the *p53* gene located on chromosome 17p are frequently observed in a variety of human cancers, including colorectal, breast, stomach, lung, and ovarian cancer. LOH is often the mechanism for the inactivation of the second allele, sometimes at an incidence approaching 100% [Lasko et al., 1991].

GENERAL MECHANISMS FOR LOH

Several mechanisms have been proposed to account for LOH, including deletion, mitotic recombination between homologous alleles, chromosome loss, and chromosome loss followed by duplication of the remaining chromosome [Bishop and Schiestl, 2001; Wijnhoven et al., 2001]. The first two, however, appear to be the major mechanisms directly associated with the loss of tumor suppressor function [Lasko et al., 1991]. These LOH events may be a consequence of the repair of DNA double-strand breaks (DSBs) occurring on the second allele, although LOH observed in human cancer may not always be initiated by DSBs. DSBs are usually repaired through either end-joining (EJ) or homologous recombination (HR; Fig. 1) [Jackson, 2002]. EJ joins sequences at broken ends with little or no homology in a nonconservative manner and results in deletions, thus potentially leading to hemizygosity. The deletion may involve the region surrounding the DSB. HR, in contrast, requires an extensive tract of sequence homology for filling the gap created by the DSB. Mitotic HR likely functions during the S/G2 phase after DNA replication, whereas EJ can occur in both G1 and S/G2 (Fig. 1) [Rothkamm et al., 2003]. Sister-chromatid recombination, as well as allelic recombination between the two chromatids of homologous chromosomes, can occur during the S/G2 phase. The former is sister-chromatid exchange (SCE) bringing about no loss or exchange of genetic information. Allelic recombination is usually error-free; however, it results in recessive mutation after chromosome segregation when the donor allele for recombination has a mutation. SCE is a major HR pathway in mammalian cells and contributes to the repair of DSBs occurring during DNA replication [Helleday, 2003]. Allelic recombination, on the other hand, repairs DSBs induced by exogenous DNA damage. LOH by HR is

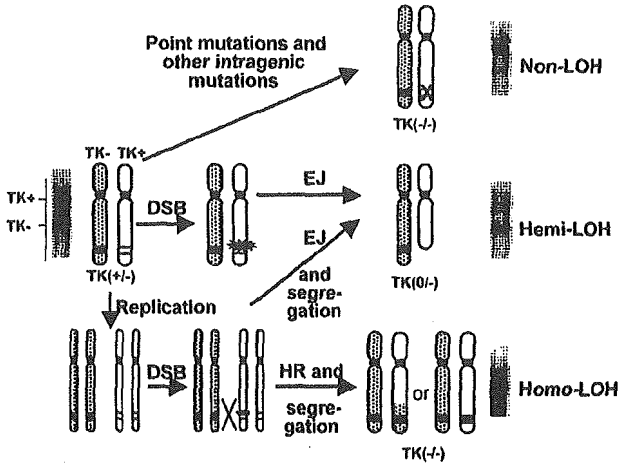

Fig. 1. A model for the mechanisms of mutation in the heterozygous *TK* gene and typical results of Southern blotting for LOH analysis. When a DSB occurs within or near the *TK* gene in G1 phase, it is repaired by EJ, resulting in hemi-LOH. A DSB generated after DNA replication is repaired by EJ or HR, leading to hemi-LOH or homo-LOH, respectively. HR operates through gene conversion with crossing-over (CO) or without CO. Quantification of the remaining allele distinguishes between hemi- and homo-LOH. A point mutation (X) does not yield LOH (non-LOH).

recognized as gene conversion with or without crossing-over (Fig. 1). Noncrossing-over involves only the localized region surrounding the DSB, while crossing-over results in a switch of the linkage relationships of all the alleles from the break point to the telomere [van Den et al., 2002].

The mechanisms of deletion and HR can explain most LOH in tumor suppressor genes during tumorigenesis. Since it is likely that the formation of large multilocus deletions involves an essential gene for cell survival located near the tumor suppressor gene, homozygous deletion may be lethal. HR does not bring about an altered phenotype as long as the first allele of the gene is functional. Thus, the consequences of deletion and HR are directly related to point mutation or other small mutations in the first allele. Independent point mutations in both alleles can also produce an altered phenotype in tumor suppressor genes. However, the frequency of this event, which varies by the type of cancer and tumor suppressor gene, is generally lower than that of LOH [Lasko et al., 1991]. This does not necessarily mean that DSBs occur more frequently than other types of DNA damage in the human genome during tumorigenesis [Loeb, 1991]. This issue will be discussed in more detail below.

EXPERIMENTAL MODELS FOR STUDYING LOH

Instead of using a tumor suppressor gene, mammalian cell models for studying LOH usually employ an endogenous autosomal gene that produces drug-resistant mutants [Wijnhoven et al., 2001]. For example, several cell lines have been engineered in which either the thymidine kinase (*TK*) gene or adenine phosphoribosyl transfer-

TABLE I. Characteristics and Spontaneous Mutant Frequencies of TK6 and Related Cell Lines

Cell lines	Status of p53	Mutation in nonfunctional *TK* allele	Mutant frequency[a] ($\times 10^{-6}$; mean ± SD) *HPRT*	*TK* (% of SG)[b]
TK6	Wild-type	CCC→CCCC at position 4,864 in exon 4	2.1 ± 2.0	3.3 ± 1.1 (64.5)
WTK-1	Homozygous mutation at codon 237 (Arg→Ile)	CC→CCC at position 4,851 in exon 4	17.4 ± 5.9	101.1 ± 6.8 (79.5)
TK6-E6	Functionally deficient by HPV-E6	Same as TK6	2.3 ± 1.8	33.5 ± 9.8 (94.0)
NH32	Null by double knockout	Same as TK6	2.7 ± 1.0	38.4 ± 9.1 (85.0)

[a]The *HPRT* and *TK* mutation assays were carried out as described by Honma et al. [1997a]. The data were obtained from at least four independent experiments.
[b]% of mutants that were of the slow-growing phenotype.

ase (*APRT*) gene is heterozygous. The remaining wild-type allele serves as the target for recessive mutation [Skopek et al., 1978; Clive et al., 1979; Fujimori et al., 1992]. A mutant clone containing the recessive mutation can be isolated by growth in the presence of a selective agent and then subjected to LOH analysis.

Mouse models, heterozygous for either the *Tk* or the *Aprt* gene, have also been developed via gene targeting in embryonic stem cells [Dobrovolsky et al., 1996; Stambrook et al., 1996]. Recessive mutations induced in vivo can be detected in cell types that can be isolated and grown in vitro, such as splenic T-lymphocytes or skin fibroblasts. Mutation has also been detected in mice using other genes, such as the T-cell receptor (*Tcr*) and some major histocompatability complex (*Mhc*) genes [Umeki et al., 1997; Kusunoki et al., 2000]. Although the frequencies of recessive mutation in these models depend on the gene target, the cell type, the animal species, and the detection system, LOH or allele loss is frequently observed in all of these model systems [Liber et al., 1987; Wijnhoven et al., 2001; Turker, 2003]. This suggests that LOH is a common mutational event in normally proliferating mammalian cells, and not only in precancerous cells during tumorigenesis.

Among these model systems, the TK6 cell line has proven useful not only for assaying gene mutation, but also for elucidating the mechanisms of LOH and DSB repair in mammalian cells [Liber et al., 1989; Li et al., 1992; Honma et al., 1997a]. TK6 and the related cell lines, WTK-1 and TK6-E6, which are p53 wild-type, p53-mutant and p53-deficient, respectively, are each heterozygous for the *TK* gene. This makes it possible to characterize the type of mutations with respect to p53 status [Morris, 2002], which is a significant advantage for studying the roles of p53 in mutation and genomic instability. The mechanisms of LOH in TK6 cells and genomic instability in the p53-deficient and p53-mutant cells have been addressed experimentally as described below.

TK6 GENE MUTATION ASSAY

The human lymphoblastoid TK6 cell line was developed by Skopek et al. [1978] for assaying *TK* gene mutation. The parent cell line of TK6 is the Epstein-Barr virus-transformed cell line WI-L2, which was originally derived from a 5-year-old male with hereditary spherocytosis. Skopek et al. [1978] first isolated a clone, HH4, which had high colony-forming efficiency without a feeder layer. They then mutagenized HH4 with ICR191 and isolated TK6, a *TK* heterozygous cell line. Later, the *TK* mutation assay using TK6 cells was optimized by Liber and Thilly [1982], evaluated extensively by many researchers, and has become one of the most popular mammalian cell gene mutation assays. TK6 cells are nearly diploid and the representative karyotype is 47, XY, 13+, t(14; 20), t(3; 21) (see Fig. 5a, later). The *TK* gene is located on the subtelomeric region of chromosome 17q. Both chromosome 17s and chromosome X appear to be normal, and TK6 cells can be used to detect *HPRT* as well as *TK* gene mutation [Liber et al., 1989]. The nonfunctional *TK* allele of TK6 cells has a single-base insertion in a three-base run of Cs in exon 4 (position 4,864) that inactivates the TK function (Table I) [Grosovsky et al., 1993]. The functional *TK* allele contains another mutation in exon 7, a single-base insertion in a four-base run of Gs (position 12,690). This frameshift mutation, however, does not affect the enzyme activity because of a substantial modification to the C-terminus of the TK protein [Giver et al., 1995].

Spontaneous mutant frequencies for the *HPRT* and *TK* genes in TK6 cells are approximately 2.1×10^{-6} and 3.3×10^{-6}, respectively [Honma et al., 1997a], which are a little lower than in vivo *HPRT* and *TK* mutant frequencies in mice or human lymphocytes (Table I) [Bigbee et al., 1998; Dobrovolsky et al., 1999]. TK6 generates two distinct phenotypic classes of *TK* mutants [Liber et al., 1989]. Normally growing (NG) mutants grow at the same rate as wild-type cells (doubling time, 13–17 hr), and the doubling time of the slowly growing (SG) mutants is greater than 21 hr. The difference is thought to be due to a putative growth-regulating gene near the *TK* gene [Amundson and Liber, 1992]. NG mutants are generally the result of small intragenic mutations such as point mutations, small deletions and small insertions, while SG mutants are associated with gross structural changes, which presumably involve the

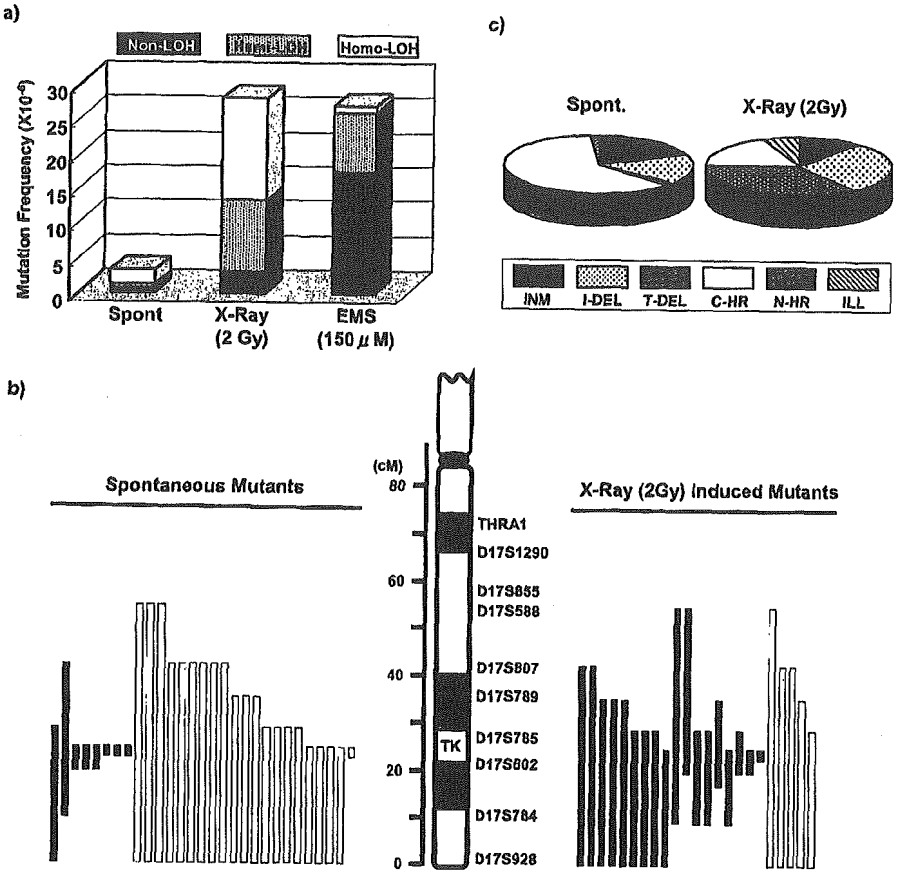

Fig. 2. Results of molecular and cytogenetic analyses of *TK* mutants in TK6 cells arising spontaneously and induced by X-rays (2 Gy) or EMS (150 μM). The procedures for the gene mutation assay and the molecular and cytogenetic analyses are described in Honma et al. [1997a] and [2000], respectively. **a:** The *TK* mutant frequency and the contribution of mutation types by LOH analysis. The mutations are classified into three types: intragenic mutations (non-LOH), hemizygous-LOH (hemi-LOH), and homozygous-LOH (homo-LOH). The type of mutation is associated with the growth phenotype of the mutants: NG and SG mutants. The percentage of each mutational event was calculated by considering the ratio of NG and SG mutants [Honma et al., 1997a]. **b:** The extent of LOH in spontaneous and X-ray-induced LOH mutants from TK6 cells. Ten microsatellite loci on the long arm of chromosome 17 that are heterozygous in TK6 cells were examined. The human *TK* locus maps to 17q23.2. Open and closed bars represent homo-LOH and hemi-LOH, respectively. The length of the bars indicates the extent of LOH. Twenty-nine spontaneous mutants (10 NG and 19 SG mutants) and 23 X-ray-induced mutants (6 NG and 17 SG mutants) were analyzed. Because the type of mutation is related to the growth phenotype of the mutants, the number of NG and SG mutants analyzed depended on the ratio of NG and SG mutants in the mutation assay [Honma et al., 1997a]. **c:** The spectrum of spontaneous and X-ray-induced mutations in the *TK* gene of TK6 cells. A combination of molecular and cytogenetic analyses revealed six types of mutation: intragenic mutation (INM), interstitial deletion (I-DEL), terminal deletion (T-DEL), homologous recombination with crossing-over (C-HR), homologous recombination without crossing-over (N-HR), and illegitimate recombination with translocation (ILL).

putative gene. The heterozygous frameshift mutations in exons 4 and 7 and another DNA polymorphism within the *TK* gene are markers for distinguishing between the functional and nonfunctional *TK* allele by Southern blot or PCR analysis and thus facilitate identification of LOH (Fig. 1) [Liber et al., 1987; Li et al., 1992; Honma et al., 2000]. Moreover, measuring the copy number of the nonfunctional *TK* allele by densitometric analysis or quantitative PCR can classify mutants with one copy of *TK* as hemizygous LOH (hemi-LOH) and those with two copies of *TK* as homozygous LOH (homo-LOH) (Fig. 1) [Li et al., 1992; Honma et al., 2000]. This LOH analysis can partially support the existence of a putative gene near the *TK* gene regulating cell growth because every SG mutant so far examined exhibits LOH [Honma et al., 1997a].

The mutational spectra of spontaneously arising *TK* mutants and those induced by X-rays and ethylmethansulfonate (EMS) are shown in Figure 2a. The majority of spontaneous *TK* mutants were of the LOH type (83%); 63% were homo-LOH and 20% were hemi-LOH. Others (17%) were non-LOH-type mutations that presumably resulted from point mutations or small intragenic mutations. It is not surprising that 83% of spontaneous mutations resulted in LOH in this assay because LOH has been detected in certain tumor suppressor genes at frequencies approaching

100% [Lasko et al., 1991]. X-rays induced predominantly LOH, while EMS induced non-LOH mutation (Fig. 2a). These results clearly indicate that X-rays cause DSBs, and that they are repaired by EJ or HR that results in LOH. In contrast, EMS produces mainly point mutation through DNA alkylation. Thus, LOH analysis of mutants obtained in the TK6 mutation assay can facilitate determining the mutagenic specificity of genotoxic agents.

LOH generally reflects multilocus events. To determine the extent of deletion and recombination, the LOH mutants were analyzed for heterozygosity at polymorphic microsatellite loci spanning chromosome 17 [Honma et al., 2000]. Figure 2b shows the position of the microsatellite loci and the extent of hemi-LOH (black bars) and homo-LOH (white bars) for spontaneous mutants and mutants induced by X-rays.

For spontaneous mutants, most of the hemi-LOH was due to small deletions that were limited to the vicinity of the *TK* gene. A small number of mutants were due to large interstitial deletions and terminal deletions, while in almost all of the homo-LOH, which results from HR with crossing-over, the deletion extended to the telomere. Only one homo-LOH mutant was of the noncrossing-over type. These results indicate that spontaneous DSBs usually are properly repaired by HR or EJ to maintain genomic integrity. X-rays mainly induced mutants with hemi-LOH in which the loss of the *TK* gene was accompanied by the loss of a large interstitial segment of the chromosome or a telomeric deletion.

These mutants were analyzed further by chromosome painting for chromosome 17. There were no remarkable chromosome changes in spontaneous LOH mutants, while shorter or translocated chromosome 17s were observed in some of the hemi-LOH mutants induced by X-rays. A shorter chromosome 17, which is defined as less than 80% of the original length, resulted from large interstitial or terminal deletions. This suggests that illegitimate recombination between nonhomologous chromosomes, as described by Richardson and Jasin [2000], may account for these chromosome alterations. The translocations were always of the unbalanced type, in which the counterpart of the translocated part of chromosome 17 containing the *TK* gene and the distal end of chromosome 17 is missing. Although terminal deletion is one of the major LOH events in X-ray-treated TK6 cells, terminal deletion was generated by neither EJ nor HR. Since TK6 and its related cell lines have high levels of telomerase activity [Neuhof et al., 2001], broken chromosomes can be stabilized by the addition of new telomere sequences, which results in the generation of terminal deletions. In other studies, we observed new telomere signals at the broken end of chromosome 17 by FISH analysis (data not shown). LOH with terminal deletion seems to be observed only in telomerase-positive immortalized cells, but not in cells in primary culture. In support of this argument, transgenic mice heterozygous for the *Aprt* (and presumably *Tk*) gene never produce terminal deletion mutants [Turker, 2003].

These molecular and cytogenetic LOH analyses have been used to construct the *TK* mutational spectrum for TK6 cells illustrated in Figure 2c. This scheme indicates that the formation of X-ray-induced mutations is distinctly different from spontaneous mutation. The gross and complicated chromosome changes observed in X-ray-induced mutants cannot be fully explained by EJ or HR repairing single DSBs that occur at the *TK* locus. Multiple DSBs clustered near the *TK* gene may be incompletely repaired and result in large interstitial or terminal deletions. Also, a type of genomic instability initiated by irradiation may affect the fidelity of DSB repair, leading to complicated DNA rearrangements.

TK6 CELL RELATIVES WITH DIFFERENT p53 STATUS

The tumor-suppressor gene *p53* is frequently mutated in a wide variety of human and rodent tumors [Levine et al., 1994]. Most cell lines established from tumors or nontumor tissues also have mutations in the *p53* gene and express either mutant or no p53 protein [Jia et al., 1997]. In fact, CHO, CHL, V79, and L5178Y cells, which are commonly used for genotoxicity tests, are all p53-mutant cell lines [Chaung et al., 1997; Clark et al., 1998; Hu et al., 1999]. This indicates that inactivation of p53 is important not only for tumorigenesis, but also for establishment of immortalized cell lines. TK6 is unusual in that this cell line has no mutations in the *p53* gene and produces only wild-type p53 protein. Further, TK6 cells respond normally to ionizing radiation-induced DNA damage, namely, they accumulate p53 protein, and the p53 downstream effectors, the $p21^{WAF-1}$ and *GADD45* genes, are induced [Little et al., 1995].

TK6 was originally derived from WI-L2 cells, which are presumably p53 wild-type (Fig. 3a). The *p53* gene in WI-L2-NS cells, also a WI-L2-derived clone, has undergone mutation from ATG to ATA in codon 237, which results in a methionine to isoleucine amino acid substitution [Zhen et al., 1995]. WI-L2-NS is homozygous for the *p53* mutation and expresses only mutant p53 protein [Zhen et al., 1995]. Since the mutated region is in a DNA sequence-specific binding site and the same mutation was observed in some human tumors [Olivier et al., 2002], the phenotype of WI-L2-NS cells may be typical of p53-mutant cells. WTK-1, which is *TK*-heterozygous, was isolated from WI-L2-NS cells by Amundson et al. [1993] for use in a *TK* mutation assay. The inactivating mutation in the nonfunctional *TK* allele is a single-base insertion in a two-base run of Cs in exon 4 (position 4,851). WTK-1 cells express approximately 10 times more p53 protein than TK6 cells because of the prolonged half-life of the

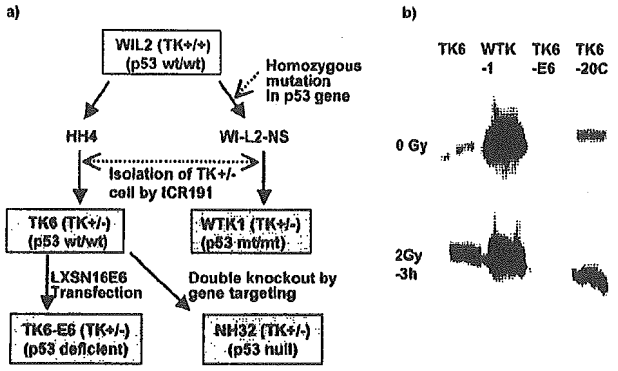

Fig. 3. Cell lineage of TK6 and related cell lines and their p53 status. **a:** TK6 and WTK-1 cells originated from the same cell line, WIL2. TK6 cells inherited a wild-type *p53* gene, while WTK-1 cells acquired homozygous *p53* mutation through WI-L2-NS cells. TK6-E6 cells are functionally p53-deficient and were established by transfection of TK6 cells with human papilloma virus E6 (HPV-E6) cDNA [Yu et al., 1997]. NH32, a *p53*-null cell, was developed by Chaung et al. [1999] by gene targeting. **b:** Western blot analysis of p53 protein in untreated and X-irradiated cells. WTK-1 cells express only mutant p53 protein, which is resistant to proteolysis and strongly accumulates in the cells. HPV-E6 abrogated expression of the p53 protein and made TK6-E6 cells functionally p53-deficient. TK6-20C is a vector control clone for HPV-E6.

mutant p53 protein (Fig. 3b) [Xia et al., 1995; Honma et al., 1997a].

TK6-E6 cells were established by transfecting TK6 cells with a vector containing full-length human papillomavirus 16 (HPV16) E6 cDNA [Yu et al., 1997]. The HPV16 E6 protein abrogates p53 function by binding and degrading it [Scheffner et al., 1990]. Western blot analysis demonstrated that TK6-E6 does not accumulate p53 protein even after X-irradiation (Fig. 3b). Thus, TK6-E6 cells can be regarded as a functionally p53-deficient cell line. Another p53-deficient cell line, NH32, was created by Chuang et al. [1999]. This is a double *p53*-knockout cell line generated by promoterless targeting of the neomycin phosphotransferase and the histidinol dehydrogenase genes into exon 2 of the *p53* gene in TK6 cells. All these cell lines are heterozygous for *TK*, are derived from the same cell line, WI-L2, and have different p53 status. Thus, characterizing these cell lines can elucidate p53-mediated biological functions, especially those involving genomic stability and DSB repair.

LOH AND GENOMIC INSTABILITY IN p53-DEFICIENT AND p53-MUTANT CELLS

The spontaneous mutant frequencies for the *HPRT* and *TK* genes of the TK6-related cell lines are shown in Table I. WTK-1, a p53-mutant cell line, exhibits an 8-fold higher spontaneous *HPRT* mutant frequency and a 30-fold higher spontaneous *TK* mutant frequency than TK6 cells [Honma et al., 1997a]. Amundson et al. [1993], who developed the WTK-1 cell line, first reported that WTK-1 cells had an approximately 30-fold higher spontaneous *TK* mutant frequency than TK6 cells, but they reported no difference in the spontaneous *HPRT* mutant frequency for the two cell lines. Recently, however, Peng et al. [2002] demonstrated an elevated spontaneous *HPRT* mutant frequency as well as *TK* mutant frequency in WTK-1 cells, corresponding to our results. In contrast, the p53-deficent cell line TK6-E6 has a 10-fold higher spontaneous *TK* mutant frequency than TK6 cells, but a similar spontaneous *HPRT* mutant frequency [Honma et al., 2000]. The *p53*-knockout cell line NH32 exhibited very similar spontaneous *TK* and *HPRT* mutant frequencies to those of TK6-E6 cells [Peng et al., 2002], although it was originally reported to show no mutator phenotype [Chuang et al., 1999]. These results indicate that both p53-deficient and p53-mutant cells are genetically unstable and have a mutator phenotype. However, since WTK-1 cells appear to be more unstable than TK6-E6 or NH32 cells, the type of mutator phenotype in the p53-deficient and p53-mutant cells must be different.

LOH analysis was used to determine the characteristics of *TK* mutations occurring in p53-deficient and p53-mutant cells (Fig. 4a). In TK6 cells, as described previously, the majority of spontaneous mutation was due to homo-LOH (63%). In TK6-E6 cells, almost all mutations were due to hemi-LOH; hemi-LOH for TK6-E6 cells was 47-fold greater than in TK6 cells, while the absolute frequencies of homo-LOH and non-LOH mutants were similar. In contrast, the increased mutant frequency in WTK1 cells was due to a substantial increase in both types of LOH (hemi-LOH, 100-fold greater than in TK6 cells; homo-LOH, 14-fold greater) and a small increase in non-LOH (5-fold greater). We conclude that LOH, but not point mutation, is primarily responsible for the mutator phenotype in both p53-deficient and p53-mutant cells.

Other studies investigating the effect of p53 on spontaneous mutant frequency, however, indicate that p53-deficient and p53-mutant cells do not have a mutator phenotype. Nishino et al. [1995] and Sands et al. [1995] found no increase in the *lacI* mutant frequency in p53-knockout mice carrying a transgenic *lacI* reporter gene. Others have reported that p53 deficiency does not affect *HPRT* and microsatellite mutant frequencies [Griffiths et al., 1997; Kazachkov et al., 1998]. The spontaneous *HPRT* mutant frequency in the p53-deficient cell line, TK6-E6, also did not increase in our studies described above. The mutation assays used in these studies, however, are biased toward detecting base substitutions, frameshifts, and other small intragenic mutations and do not efficiently detect large deletions and other gross structural changes. Thus, the failure in these studies to demonstrate a mutator phenotype in p53-deficient cells and mice is likely due to the limitations of the gene mutation assay systems employed.

Figure 4b shows LOH mapping on chromosome 17 for the spontaneous LOH mutants from TK6-E6 and WTK-1

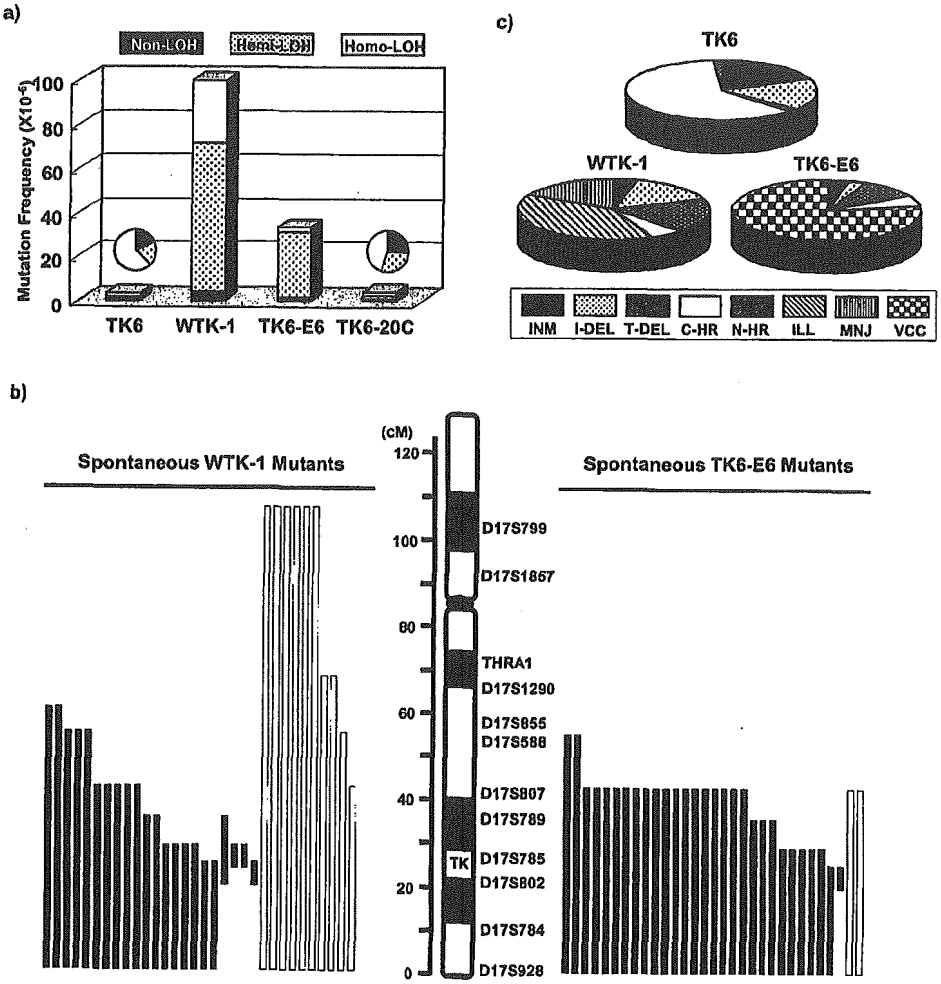

Fig. 4. Results of molecular and cytogenetic analyses of spontaneous *TK* mutants from WTK-1 (p53-mutant) and TK6-E6 (p53-deficient) cells. The procedures are described in Honma et al. [1997a, 2000] and in the legend to Figure 2. **a:** The spontaneous *TK* mutant frequency and the contribution of mutation type by LOH analysis. The percentage of each mutational event was calculated by considering the ratio of NG and SG mutants (Table I). **b:** Extent of LOH in spontaneous LOH mutants from WTK-1 and TK6-E6 cells. Twelve microsatellite loci on the long and short arm of chromosome 17 were examined. Thirty-two WTK-1 mutants (7 NG and 25 SG mutants) and 31 TK6-E6 mutants (2 NG and 29 SG mutants) were analyzed. The number of NG and SG mutants analyzed depended on the ratio of NG and SG mutants in the mutation assay (Table I). Open and closed bars represent homo- and hemi-LOH, respectively. **c:** Spectra of spontaneous *TK* mutation in TK6, WTK-1, and TK6-E6 cells. Eight types of mutations were recognized in the cell lines: intragenic mutation (INM), interstitial deletion (I-DEL), terminal deletion (T-DEL), homologous recombination with crossing-over (C-HR), homologous recombination without crossing-over (N-HR), illegitimate recombination with translocation (ILL), whole chromosome loss followed by duplication through mitotic nondisjunction (MNJ), and various chromosome changes (VCC). Redrawn from Honma et al. [1997a, 2000].

cells. WTK-1 mutants had hemi-LOH as well as homo-LOH extending to the end of chromosome 17. LOH at microsatellite markers on both the short and long arms of chromosome 17 was detected in approximately half of the homo-LOH mutants, suggesting that whole chromosome loss followed by chromosome duplication contributed to the generation of homo-LOH WTK-1 mutants. As no LOH mutants due to whole chromosome loss have been observed in TK6 or TK6-E6 cells, the mutant form of p53 protein may initiate another type of genomic instability, presumably through a defect in mitosis [Tarapore and Fukasawa, 2000].

Chromosome painting analysis supported this hypothesis (Fig. 5); mutants with LOH at every locus analyzed on chromosome 17 had no structural changes in the chromosome. The cytogenetic analysis also revealed that 50% of hemi-LOH and 20% of homo-LOH involved an unbalanced translocation, indicating that WTK-1 cells may have abnormal recombination capacity [Honma et al., 1997b]. The homo-LOH mutants with the unbalanced translocation gained an additional chromosome 17, resulting in partial trisomy of chromosome 17 (Fig. 5b). Since aneuploidy was not always observed in every metaphase in a mutant clone, it may be generated after the induction

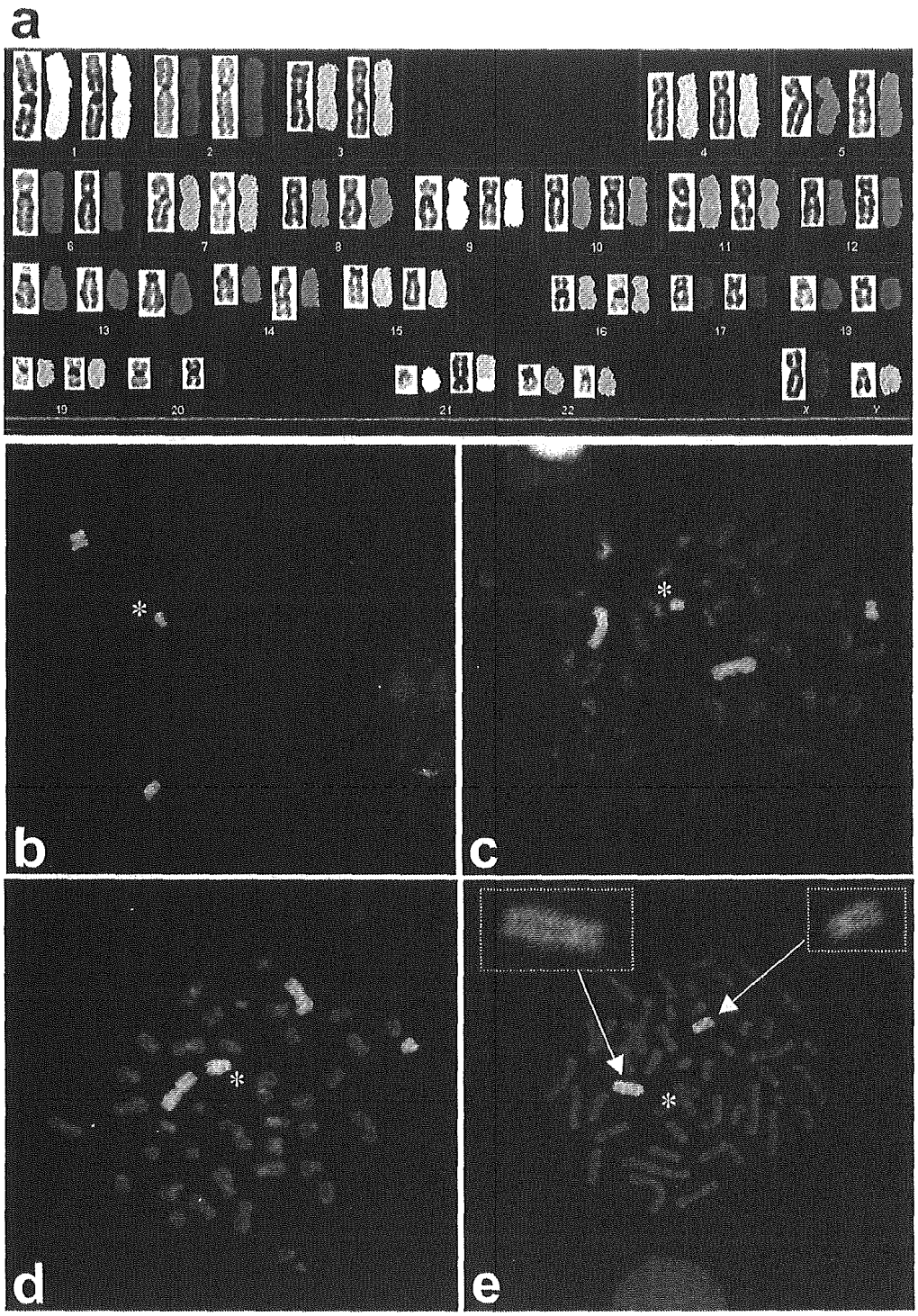

Fig. 5. Cytogenetic analysis of TK6 cells and *TK* mutants from related cell lines. Detailed procedures for chromosome painting analysis and spectral karyotype (SKY) analysis are described in Honma et al. [2000] and [2002], respectively. **a:** SKY analysis of TK6 cells. The representative karyotype is 47, XY, 13+, t(14; 20), t(3; 21). **b:** Chromosome 17 (yellow) painting analysis of a *TK* mutant from WTK-1 cells. This mutant has an unbalanced translocation accompanied by partial trisomy of chromosome 17. Reproduced with permission from Honma et al. [1997b]. **c–e:** A variety of chromosome changes in *TK* mutants from TK6-E6 cells. Deletion (c), translocation (d), and gene amplification (e) of chromosome 17 (green) heterogeneously appear as a mosaic in these mutants. Reproduced with permission from Honma et al. [2000].

of a translocation as a compensation for the partial loss of chromosome 17. Gain of a chromosome 17 may be associated with the mitotic defect in WTK-1 cells [Honma et al., 1997b]. Thus, WTK-1 cells are likely to have two types of genomic instability. The first involves abnormal or illegitimate recombination leading to translocation. The second is a mitotic defect increasing the probability of generating aneuploidy through aberrant segregation. Both mechanisms could contribute to the elevated spontaneous *TK* mutant frequency in WTK-1 cells.

Almost all spontaneous *TK* mutants in TK6-E6 cells were due to hemi-LOH extending from the breakpoint to the end of chromosome 17 (Fig. 4b) [Honma et al., 2000]. Chromosome painting analysis revealed that most of the hemi-LOH mutants contained apparent structural changes in chromosome 17, including deletion, translocation, and gene amplification. Thus, a portion of the long arm of chromosome 17 is elongated (Fig. 5c–e) [Honma et al., 2000]. Importantly, these chromosome changes were not observed in every cell of the mutant clone, but appeared heterogeneously as a mosaic in a given mutant clone. This suggests that multiple chromosome changes occurred that were not directly related to the initial *TK* mutation, but occurred independently in each cell during clonal expansion. We speculate that inappropriate repair of spontaneous DSBs results in the chromosome changes through a breakage-fusion-bridge (BFB) cycle (Fig. 6).

In wild-type p53 cells, a spontaneous DSB occurring in G1 phase is appropriately repaired by EJ, or cells having unrepaired DSBs are eliminated by the p53-dependent G1/S checkpoint and apoptosis [Wiesmuller, 2001]. A TK6-E6 cell with an unrepaired DSB, however, can escape from the checkpoint and enter into S-phase with a broken chromosome. After DNA replication, the broken sister chromatids may fuse with each other to form a chromatid bridge. The dicentric chromatid would be torn apart at cell division, producing daughter cells with broken chromosomes again, thereby perpetuating the BFB cycle [Coquelle et al., 1997; Pipiras et al., 1998]. If the dicentric chromatid was separated asymmetrically, one daughter cell would receive a shortened chromosome and the other an elongated one. Occasionally, the broken chromatids may be stabilized with another chromosome fragment by EJ, leading to a translocation (Fig. 6). Consequently, the genetic changes sequentially accumulate as a mosaic of chromosome aberration during cell growth. Thus, the cause of the mutator phenotype and genomic instability in TK6-E6 cells is likely to be unrepaired DSBs that have escaped the G1/S checkpoint. This could trigger the BFB cycle, resulting in LOH with multiple chromosome alterations.

The molecular and cytogenetic analysis of LOH mutants in these studies revealed a variety of mechanisms leading to LOH (Fig. 7). Class I (hemi-LOH) and class II (homo-LOH) mechanisms are thought to be the consequence of

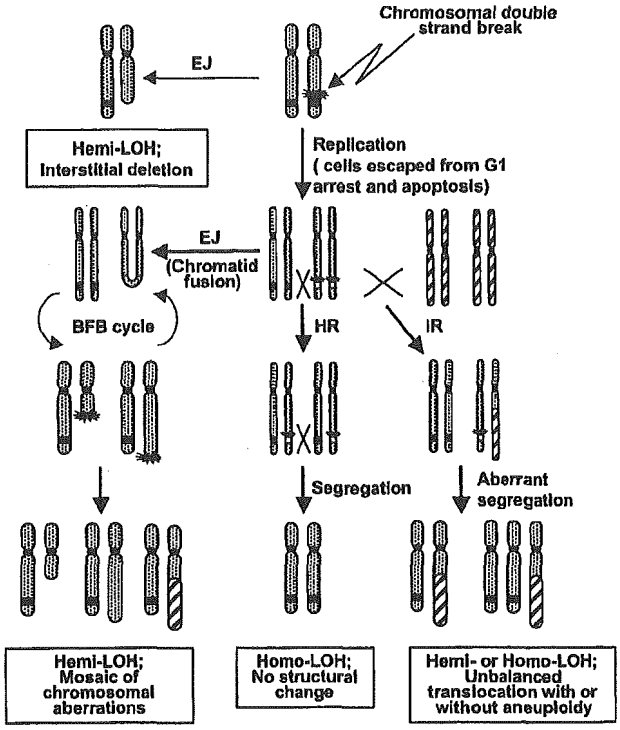

Fig. 6. A model for mechanisms that elicit DSB repair in p53-deficient (TK6-E6) and p53-mutant (WTK-1) cells. A DSB occurring in G1 phase is repaired by EJ resulting in interstitial deletion. Some cells containing unrepaired DSBs escape from the p53-dependent G1 checkpoint and apoptosis to enter S-phase and generate a pair of chromatid breaks. In TK6-E6 cells, the chromatid breaks fuse with each other, forming a chromatid bridge and triggering the BFB cycle, thereby resulting in multiple chromosome changes, including deletion, amplification, and translocation. In WTK-1 cells, the broken chromatids are preferably repaired by illegitimate recombination as well as HR leading to homo- or hemi-LOH, with or without a translocation because of the cell's hyper but unfaithful recombination capacity. The mitotic defect in WTK-1 cells generates hemi-LOH with partial trisomy through aberrant segregation. Redrawn from Honma et al. [1997b].

DSBs repaired in a conservative or nonconservative manner. Class III (involving the whole chromosome) is associated with a mitotic disturbance. Figure 4c shows the spectra for spontaneous *TK* mutations in TK6-E6 and WTK-1 cells. Although both the p53-deficient and p53-mutant cells exhibited a mutator phenotype and predominantly produce LOH, the mechanisms are distinctly different in the two cell lines.

ROLE OF p53 IN MAINTAINING GENOMIC STABILITY

The p53 tumor suppressor protein is regarded as the guardian of the genome because it appears to be important in maintaining genomic stability in mammalian cells [Lane, 1992]. It mediates certain cellular responses following DNA damage and plays a role in G1 arrest and apoptosis [Weinert and Lydall, 1993]. It has been

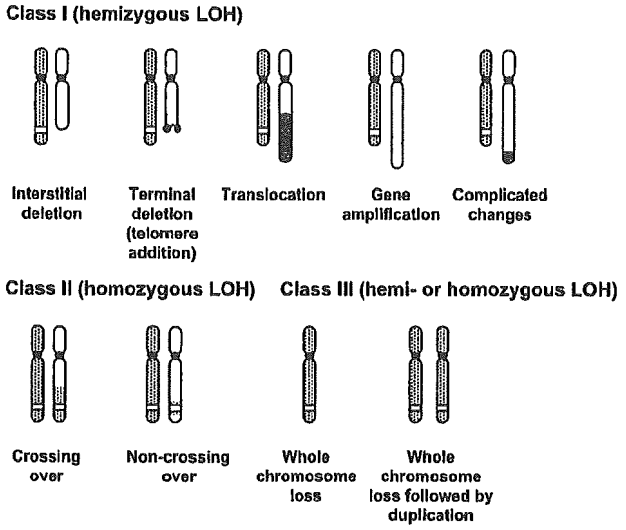

Fig. 7. Types of LOH observed in TK6 cells and related cell lines. The class I type is involved in structural chromosome changes. The class II type results from HR in a conservative manner. The class III type is associated with a mitotic defect leading to numerical chromosome changes. The class III type sometimes combines with the class I type.

hypothesized that G1 arrest allows cells time to repair DNA damage prior to DNA replication, while apoptosis serves to eliminate potentially oncogenic cells [Kuerbitz et al., 1992; Selivanova and Wiman, 1995]. Based on this hypothesis, one would predict that p53-inactivated cells would be more likely to become malignant than p53 wild-type cells. This would result from cells having unrepaired DNA damage, escaping apoptosis, and continuing to divide and accumulate mutations. Both WTK-1 and TK6-E6 cells do not express *p21* [Yu et al., 1997], which mediates G1 arrest through p53 regulation [Zhang et al., 1993]. This suggests that both cell lines have a defect in the G1/S checkpoint. Following irradiation, TK6-E6 cells display a delayed apoptotic response and WTK-1 cells exhibit not only a delayed but also a reduced apoptotic response. In contrast, TK6 cells rapidly undergo apoptosis [Little et al., 1995; Xia et al., 1995; Yu et al., 1997]. These observations indicate that the failure of the G1 checkpoint and apoptosis may partially contribute to the accumulation of mutations in p53-deficient and p53-mutant cells. However, these deficiencies cannot fully explain the genomic instability and increased tumorigenicity of p53-inactivated cells. For example, exposure to a chemical that inhibits p53-mediated apoptosis does not lead to tumor formation in mice [Komarov et al., 1999], and *p21*-knockout mice do not develop spontaneous tumors [Deng et al., 1995]. Thus, another mechanism, presumably abnormal DNA repair, also contributes to genomic instability leading to tumor development in p53-inactivated cells.

Inactivation of p53 also enhances the rate of gene amplification [Livingstone et al., 1992; Tlsty, 2002], produces structural and numerical chromosome changes [Agapova et al., 1996; Lengauer et al., 1998], and deregulates centrosomal replication leading to abnormal chromosomal segregation [Tarapore and Fukasawa, 2000]; but p53 inactivation does not affect the accumulation of point mutations [Lu and Lane, 1993]. These observations are consistent with our findings that a high percentage of the mutant fraction in both p53-mutant and p53-deficient cells occurs from LOH due to structural and/or numerical chromosome changes. We propose that altered DSB repair mechanisms, probably HR, and/or mitotic disturbances cause the genomic instability in WTK-1 and/or TK6-E6 cells.

Evidence is accumulating that p53 plays an important role in other DNA repair pathways, such as nucleotide excision repair (NER) [Mathonnet et al., 2003], base excision repair (BER) [Zurer et al., 2004], and maintenance of the nucleotide pool through the ribonucleotide reductase activity of p53R2 [Tanaka et al., 2000]. Defects in these repair pathways, however, seem to affect the accumulation of point mutations, but not gross chromosomal changes [van Steeg et al., 2000; Kimura et al., 2003]. Since NER functions to remove many types of DNA lesions, a defect or modification of the NER machinery may result in mutations due to DNA lesions such as those induced by UV light, bulky adducts, and DNA crosslinks. The spontaneous mutation frequency, however, would not be affected by reduced NER function [van Kreijl et al., 2001; van Steeg, 2001]. Although a contribution of NER to the mutator phenotypes cannot be fully excluded, the mutator phenotypes in untreated WTK-1 and TK6-E6 cells are probably independent of NER.

Many studies have addressed the association between p53 and HR, and almost all have concluded that wild-type p53 represses HR and that both p53-deficient and p53-mutant cells show high recombination activity [Bertrand et al., 1997; Mekeel et al., 1997; Akyuz et al., 2002]. This conclusion is in contrast to the results from our series of studies: p53 wild-type TK6 cells have normal recombination activity leading to homo-LOH; p53-mutant WTK-1 cells produce homo-LOH, as well as homo-LOH combined with translocations due to an increased level of abnormal recombination activity; and p53-deficient TK6-E6 cells do not have an increased frequency of homo-LOH by HR.

Other studies measuring HR primarily used an artificial reporter substrate based on an exogenous drug-resistance gene. These models are designed to detect intermolecular recombination between the substrates or intramolecular recombination between tandem repeat sequences within the substrate [Bertrand et al., 2004]. These systems detect not only conservative gene conversion, but also deleterious changes that occur in a nonconservative manner. Loss of wild-type p53 and expression of a mutant p53 protein enhance the recombination frequency in cells containing these types of recombination substrates, while

expression of wild-type p53 suppresses the recombination frequency [Akyuz et al., 2002; Saintigny and Lopez, 2002]. Xia et al. [1994], using a transfection assay with plasmid recombination substrates, demonstrated that WTK-1 cells have a sevenfold higher intermolecular recombination frequency than TK6 cells. A high capacity for intramolecular recombination in WTK-1 cells has also been demonstrated in an *HPRT* minigene with a duplication of exon 2 and a tandem repeat recombination substrate integrated into the genome [Gebow et al., 2000; Akyuz et al., 2002]. Some mutant p53 proteins, including that expressed in WTK-1 cells, however, seem to enhance not only HR, but also illegitimate recombination. Recombination between substrates with low homology was also induced at a similar level in these studies [Gebow et al., 2000; Akyuz et al., 2002].

Although p53-deficient cells also exhibit high recombination capacity in the HR assays, it is not clear whether interallelic HR leading to LOH is influenced by the loss of p53 function. Shao et al. [2000] developed p53-deficient $Aprt^{+/-}$ mice and examined mechanisms of LOH in the *Aprt* gene of skin fibroblasts and T-lymphocytes. The p53-deficient mice produced about three times more *Aprt* mutant fibroblasts than wild-type mice. Molecular analysis revealed that the majority of the *Aprt* mutants in both the p53-deficient and p53 wild-type mice resulted from LOH caused by HR. However, the increased frequency of LOH in the p53-deficient mice was not necessarily due to HR and sometimes was due to deletion. The LOH due to deletion was enhanced by radiation exposure more efficiently in p53-deficent mice than p53 wild-type mice [Liang et al., 2002]. These studies provide no evidence that LOH can be efficiently induced through HR in p53-deficient mice. As TK6-E6 cells produced homo-LOH at a level similar to that seen in TK6 cells, HR must operate effectively in TK6-E6 cells and therefore is not directly associated with the mutator phenotype.

DSBs occurring in the G1 phase are mainly repaired by EJ [Rothkamm et al., 2003]. If they cannot be repaired, the p53-dependent G1/S checkpoint and apoptosis will eliminate the unrepaired cells to prevent their entering S-phase [Weinert and Lydall, 1993]. In TK6-E6 and WTK-1 cells, however, some of the cells may have escaped this surveillance system (Fig. 6). The DSBs generated through DNA replication presumably are repaired by either HR or EJ during late S/G2 phase. In WTK-1 cells, both HR and illegitimate recombination are operational and result in homo-LOH and hemi-LOH with accompanying translocations [Honma et al., 1997b]. In TK6-E6 cells, however, EJ functions to repair broken chromatids and form a chromatid bridge perpetuating the BFB cycle [Honma et al., 2000]. We recently demonstrated that EJ, but not HR, repairs the breakage of both sister chromatids even after DNA replication [Honma et al., 2003]. Thus, it is likely that DSBs that escape the surveillance system initiate genomic instability in both TK6-E6 and WTK-1 cells; moreover, the abnormal recombination capacity in WTK-1 cells enhances the instability.

Considering the apparent differences in the mutator phenotypes of WTK-1 and TK6-E6 cells, we hypothesized that the mutant p53 protein (Ile237) expressed in WTK-1 cells has a dominant-negative effect that causes genomic instability through an abnormal recombination capacity. Xia and Liber [1997] demonstrated that overexpressing mutant p53 protein (Ile237 or Ala143) in TK6 cells increased the spontaneous *TK* mutant frequency to 10–40 $\times$ 10^{-6}, which is intermediate between the mutant frequencies of TK6 and WTK-1 cells. The human lymphoblastoid AHH-1/$TK^{+/-}$ and MCL-5 cell lines, which were established by Crespi and Thilly [1984], both originated from AHH-1 cells and both can be used for assaying *TK* mutation. MCL-5 is a p53 wild-type cell line, while AHH-1 is heterozygous for the *p53* gene and expresses both wild-type and mutant (282Trp) p53 protein [Morris et al., 1996]. The spontaneous *TK* mutant frequency in AHH-1 cells is about 17 $\times$ 10^{-6}, which is fivefold higher than that of MCL-5 cells [Dobo et al., 1995]. Molecular analysis revealed that 96% of spontaneous *TK* AHH-1 mutants and 47% of spontaneous MCL-5 mutants contained LOH, although homo-LOH and hemi-LOH were not distinguished [Dobo et al., 1997]. Thus, the heterozygous p53-mutant cell line, AHH-1, appears to have an intermediate mutator phenotype between TK6 and WTK-1 cells. The p53 protein is known to be a tetramer, and at least three mutant proteins are required to express a dominant-negative effect efficiently [Chan et al., 2004]. This suggests that *p53* heterozygous cells may have a weak mutator phenotype because of attenuation by wild-type p53 protein.

Another type of genomic instability associated with p53 inactivation is mitotic disturbance. A number of studies have shown a strong correlation between the inactivation of p53 and ploidy changes [Tarapore and Fukasawa, 2000]. Cytogenetic analyses clearly demonstrate that embryonic fibroblasts and tumor tissues from $p53^{-/-}$ mice exhibit a high degree of aneuploidy [Fukasawa et al., 1996; Liu et al., 2004]. We found that aneuploid cells, which were recognized as gain of a chromosome 17, often appear in WTK-1 LOH mutants, but not in LOH mutants from TK6 or TK6-E6 cells. One of the mechanisms for aneuploidy is abnormal amplification of the centrosome, leading to an increased frequency of defective mitoses due to the multiple spindle poles and resulting in missegregation of chromosomes into the daughter cells [Fukasawa et al., 1996]. This mechanism can be induced by p53 inactivation. Even though aneuploidy associated with centrosome amplification is a characteristic of typical p53-deficient cells, some mutant p53 cell lines do not show an enhancement of aneuploid cells via centrosome amplification [Liu et al., 2004]. Again, this contrasts with

our results. Because LOH arising through aneuploidy in our system must be initiated by the loss of a chromosome, another mechanism, such as the premature initiation of mitosis by the loss of the G2/M transition checkpoint, probably is involved in the generation of aneuploidy in WTK-1 cells [Tarapore and Fukasawa, 2000].

MUTATION SPECTRUM DOES NOT NECESSARILY CORRESPOND WITH MECHANISM OF MUTATION

It is well known that almost all DSBs are repaired by EJ in mammalian cells, and that even when HR is involved, it is principally the noncrossing-over type of recombination [Stark and Jasin, 2003]. In the *TK* mutational spectrum of TK6 cells, however, most of the spontaneous LOH mutants resulted from HR with crossing-over (Fig. 2c). This apparent discrepancy is due to the strong bias for recovery of HR with crossing-over in mutation assays involving recessive genes (Fig. 7). DSBs occurring within the *TK* gene can be recovered by any repair pathway as *TK*-deficient mutants (Fig. 8a). When DSBs are generated outside the *TK* gene, however, HR with crossing-over and terminal loss by deletion or translocation can recover the DSB as a mutant, but EJ and HR without crossing-over cannot (Fig. 8b). This is because these two later mechanisms are localized events that do not affect the *TK* gene. In fact, almost all spontaneous homo-LOH mutants in TK6 cells had LOH from > 5 cM proximal of the *TK* gene to the end of chromosome 17 (Fig. 2b), indicating that most DSBs that occur outside of the *TK* gene were recovered by HR with crossing-over or terminal loss.

The target size for the recoverable DNA damage totally depends on the type of mutation [Quintana et al., 2001]. When the spectrum of spontaneous *TK* mutation in TK6 cells shown in Figure 2c is reevaluated as yield per kb, point mutations and small interstitial deletions are the major mutational events [Loeb, 1991], and noncrossing-over HR occurs more frequently than the crossing-over type [Quintana et al., 2001]. Any gene mutation assay is biased to detect specific mutations; the *TK* and *APRT* gene mutation assays are biased to detect HR with crossing-over [Wijnhoven et al., 2001; Turker, 2003], whereas the *HPRT* and transgenic *lacZ* and *lacI* gene mutation assays mainly detect point mutations and small deletions [Gossen et al., 1989; Kohler et al., 1991]. It is important to keep in mind the limitations of the information generated from mutation assay systems. The mutation spectra generated from untargeted mutagenesis do not quantitatively correspond with mutation or repair mechanisms, although they must be relevant for genetic changes in human tumorigenesis.

Recently, we developed a system to trace the fate of a DSB occurring in the TK6 cell *TK* gene, in which a meganuclease I-*Sce*I site is integrated into the *TK* gene

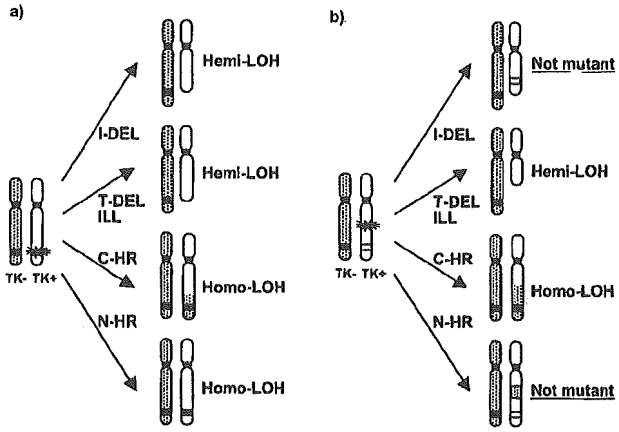

Fig. 8. The *TK* mutation assay is biased to recover specific types of mutations in untargeted mutagenesis. **a:** DSBs occurring within the *TK* gene result in *TK* mutants by any pathway: interstitial deletion (I-DEL), terminal deletion or translocation (T-DEL, ILL), HR with crossing-over (C-HR), and HR without crossing-over (N-HR). **b:** When DSBs occur outside of the *TK* gene, I-DEL and N-HR do not result in *TK* mutants.

and a specific DSB is generated at the site by expressing the I-*Sce*I enzyme [Honma et al., 2003]. Unlike untargeted mutagenesis, this system makes it possible to evaluate the relative contribution of EJ and HR in the repair of DSBs without bias. This study clearly demonstrated that almost all DSBs were repaired by EJ, and that a minor portion was repaired by HR with noncrossing-over, supporting the preference of the mammalian DSB repair pathway commonly reported.

CONCLUSION

Since LOH is frequently observed in tumor suppressor genes from various kinds of human tumors, LOH is considered to be a critical genetic event during human carcinogenesis. LOH is thought to be a consequence of the repair of DSBs; EJ causes interstitial deletions resulting in hemi-LOH, while HR between homologous alleles generates homo-LOH. These repair mechanisms seem to be important in maintaining genomic stability rather than the induction of genomic instability in mammalian cells. Ideally, DSBs occurring in the mammalian genome are repaired in a manner that minimizes gross genetic changes. In particular, HR is error-free and does not cause any genetic changes as long as the donor sequence for recombination has no mutation. Thus, LOH is not necessarily a detrimental event when the HR pathway functions correctly.

p53 appears to be important in maintaining the genomic stability associated with DSB repair because inactivation of p53 enhances the frequency of LOH and changes the balance between hemi-LOH and homo-LOH. Both p53-deficient TK6-E6 cells and p53-mutant WTK-1 cells have defects in the G1 checkpoint and in apoptosis, which form a critical guard system for eliminating potentially cancerous

cells. Unrepaired cells may escape this surveillance system and enter S-phase; after DNA replication, the unrepaired DSBs can initiate genomic instability. The pair of broken chromatids generated by DNA replication can fuse to each other, forming a chromatid bridge and triggering the BFB cycle. This can then result in a variety of chromosome changes in the cell, because EJ operates primarily on the broken chromatids even during the S/G2 phase. In p53-mutated WTK-1 cells, the genomic instability is enhanced since the mutant p53 protein (Ile237) has a dominant-negative effect for HR. The broken chromatids in WTK-1 cells are preferentially repaired by illegitimate recombination as well as by HR, leading to translocations because of an abnormal recombination activity. Moreover, WTK-1 cells have the ability to undergo abnormal mitosis, thus generating LOH through aneuploidy.

Overall, the generation of LOH and its associated genomic instability strongly depend on p53 status. Most LOH is initiated by DSBs and their elimination and repair is mediated by functions of the wild-type p53 protein.

ACKNOWLEDGMENTS

The human cell lines used in the studies were kindly supplied by Dr. John B. Little of the Harvard School of Public Health, Boston, MA, and Howard L. Liber, now of Colorado State University, Ft. Collins, CO.

REFERENCES

Agapova LS, Ilyinskaya GV, Turovets NA, Ivanov AV, Chumakov PM, Kopnin BP. 1996. Chromosome changes caused by alterations of p53 expression. Mutat Res 354:129–138.

Akyuz N, Boehden GS, Susse S, Rimek A, Preuss U, Scheidtmann KH, Wiesmuller L. 2002. DNA substrate dependence of p53-mediated regulation of double-strand break repair. Mol Cell Biol 22:6306–6317.

Amundson SA, Liber HL. 1992. A comparison of induced mutation at homologous alleles of the *tk* locus in human cells: II, molecular analysis of mutants. Mutat Res 267:89–5.

Amundson SA, Xia F, Wolfson K, Liber HL. 1993. Different cytotoxic and mutagenic responses induced by X-rays in two human lymphoblastoid cell lines derived from a single donor. Mutat Res 286:233–241.

Bertrand P, Rouillard D, Boulet A, Levalois C, Soussi T, Lopez BS. 1997. Increase of spontaneous intrachromosomal homologous recombination in mammalian cells expressing a mutant p53 protein. Oncogene 14:1117–1122.

Bertrand P, Saintigny Y, Lopez BS. 2004. p53's double life: transactivation-independent repression of homologous recombination. Trends Genet 20:235–243.

Bigbee WL, Fuscoe JC, Grant SG, Jones IM, Gorvad AE, Harrington-Brock K, Strout CL, Thomas CB, Moore MM. 1998. Human in vivo somatic mutation measured at two loci: individuals with stably elevated background erythrocyte glycophorin A (gpa) variant frequencies exhibit normal T-lymphocyte *hprt* mutant frequencies. Mutat Res 397:119–136.

Bishop AJ, Schiestl RH. 2001. Homologous recombination as a mechanism of carcinogenesis. Biochim Biophys Acta 1471:M109–M121.

Cavenee WK, Dryja TP, Phillips RA, Benedict WF, Godbout R, Gallie BL, Murphree AL, Strong LC, White RL. 1983. Expression of recessive alleles by chromosomal mechanisms in retinoblastoma. Nature 305:779–784.

Cavenee WK, Hansen MF, Nordenskjold M, Kock E, Maumenee I, Squire JA, Phillips RA, Gallie BL. 1985. Genetic origin of mutations predisposing to retinoblastoma. Science 228:501–503.

Chan WM, Siu WY, Lau A, Poon RY. 2004. How many mutant p53 molecules are needed to inactivate a tetramer? Mol Cell Biol 24:3536–3551.

Chaung W, Mi LJ, Boorstein RJ. 1997. The p53 status of Chinese hamster V79 cells frequently used for studies on DNA damage and DNA repair. Nucl Acids Res 25:992–994.

Clark LS, Hart DW, Vojta PJ, Harrington-Brock K, Barrett JO, Moore MM, Tindal KR. 1998. Identification and chromosomal assignment of two heterozygous mutations in the Trp53 gene in L5178Y(+/−)-3.7.2C mouse lymphoma cells. Mutagenesis 15:427–434.

Chuang YY, Chen Q, Brown JP, Sedivy JM, Liber HL. 1999. Radiation-induced mutations at the autosomal thymidine kinase locus are not elevated in p53-null cells. Cancer Res 59:3073–3076.

Clive D, Johnson KO, Spector JF, Batson AG, Brown MM. 1979. Validation and characterization of the L5178Y/$TK^{+/-}$ mouse lymphoma mutagen assay system. Mutat Res 59:61–108.

Coquelle A, Pipiras E, Toledo F, Buttin G, Debatisse M. 1997. Expression of fragile sites triggers intrachromosomal mammalian gene amplification and sets boundaries to early amplicons. Cell 89:215–225.

Crespi CL, Thilly WG. 1984. Assay for gene mutation in a human lymphoblast line, AHH-1, competent for xenobiotic metabolism. Mutat Res 128:221–230.

Deng C, Zhang P, Harper JW, Elledge SJ, Leder P. 1995. Mice lacking p21CIP1/WAF1 undergo normal development, but are defective in G1 checkpoint control. Cell 82:675–684.

Dobo KL, Giver CR, Eastmond DA, Rumbos HS, Grosovsky AJ. 1995. Extensive loss of heterozygosity accounts for differential mutation rate on chromosome 17q in human lymphoblasts. Mutagenesis 10:53–58.

Dobo KL, Eastmond DA, Grosovsky AJ. 1997. The influence of cellular apoptotic capacity on N-nitrosodimethylamine-induced loss of heterozygosity mutations in human cells. Carcinogenesis 18:1701–1707.

Dobrovolsky VN, Casciano DA, Heflich RH. 1996. Development of a novel mouse $tk^{+/-}$ embryonic stem cell line for use in mutagenicity studies. Environ Mol Mutagen 28:483–489.

Dobrovolsky VN, Casciano DA, Heflich RH. 1999. $Tk^{+/-}$ mouse model for detecting in vivo mutation in an endogenous, autosomal gene. Mutat Res 423:125–136.

Fujimori A, Tachibana A, Tatsumi K. 1992. Allelic losses in mutations at the aprt locus of human lymphoblastoid cells. Mutat Res 269:55–62.

Fukasawa K, Choi T, Kuriyama R, Rulong S, Vande Woude GF. 1996. Abnormal centrosome amplification in the absence of p53. Science 271:1744–1747.

Gebow D, Miselis N, Liber HL. 2000. Homologous and nonhomologous recombination resulting in deletion: effects of p53 status, microhomology, and repetitive DNA length and orientation. Mol Cell Biol 20:4028–4035.

Giver CR, Nelson SL Jr, Cha MY, Pongsaensook P, Grosovsky AJ. 1995. Mutational spectrum of X-ray induced TK^{-} human cell mutants. Carcinogenesis 16:267–275.

Gnarra JR, Tory K, Weng Y, Schmidt L, Wei MH, Li H, Latif F, Liu S, Chen F, Duh FM. 1994. Mutations of the VHL tumour suppressor gene in renal carcinoma. Nat Genet 7:85–90.

Gossen JA, de Leeuw WJ, Tan CH, Zwarthoff EC, Berends F, Lohman PH, Knook DL, Vijg J. 1989. Efficient rescue of integrated shuttle vectors from transgenic mice: a model for studying mutations in vivo. Proc Natl Acad Sci USA 86:7971–7975.

Griffiths SD, Clarke AR, Healy LE, Ross G, Ford AM, Hooper ML, Wyllie AH, Greaves M. 1997. Absence of p53 permits propagation of mutant cells following genotoxic damage. Oncogene 14:523–531.

Grosovsky AJ, Walter BN, Giver CR. 1993. DNA-sequence specificity of mutations at the human thymidine kinase locus. Mutat Res 289:231–243.

Helleday T. 2003. Pathways for mitotic homologous recombination in mammalian cells. Mutat Res 532:103–115.

Honma M, Hayashi M, Sofuni T. 1997a. Cytotoxic and mutagenic responses to X-rays and chemical mutagens in normal and p53-mutated human lymphoblastoid cells. Mutat Res 374:89–98.

Honma M, Zhang LS, Hayashi M, Takeshita K, Nakagawa Y, Tanaka N, Sofuni T. 1997b. Illegitimate recombination leading to allelic loss and unbalanced translocation in p53-mutated human lymphoblastoid cells. Mol Cell Biol 17:4774–4781.

Honma M, Momose M, Tanabe H, Sakamoto H, Yu Y, Little JB, Sofuni T, Hayashi M. 2000. Requirement of wild-type p53 protein for maintenance of chromosomal integrity. Mol Carcinog 28:203–214.

Honma M, Tadokoro S, Sakamoto H, Tanabe H, Sugimoto M, Furuichi Y, Satoh T, Sofuni T, Goto M, Hayashi M. 2002. Chromosomal instability in B-lymphoblasotoid cell lines from Werner and Bloom syndrome patients. Mutat Res 520:15–24.

Honma M, Izumi M, Sakuraba M, Tadokoro S, Sakamoto H, Wang W, Yatagai F, Hayashi M. 2003. Deletion, rearrangement, and gene conversion; genetic consequences of chromosomal double-strand breaks in human cells. Environ Mol Mutagen 42:288–298.

Hu T, Miller CM, Ridder GM, Aardema MJ. 1999. Characterization of p53 in Chinese hamster cell lines CHO-K1, CHO-WBL, and CHL: implications for genotoxicity testing. Mutat Res 426:51–62.

Jackson SP. 2002. Sensing and repairing DNA double-strand breaks. Carcinogenesis 23:687–696.

Jia LQ, Osada M, Ishioka C, Gamo M, Ikawa S, Suzuki T, Shimodaira H, Niitani T, Kudo T, Akiyama M, Kimura N, Matsuo M, Mizusawa H, Tanaka N, Koyama H, Namba M, Kanamaru R, Kuroki T. 1997. Screening the p53 status of human cell lines using a yeast functional assay. Mol Carcinog 19:243–253.

Kazachkov Y, Yoffe B, Khaoustov VI, Solomon H, Klintmalm GB, Tabor E. 1998. Microsatellite instability in human hepatocellular carcinoma: relationship to p53 abnormalities. Liver 18:156–161.

Kimura T, Takeda S, Sagiya Y, Gotoh M, Nakamura Y, Arakawa H. 2003. Impaired function of p53R2 in Rrm2b-null mice causes severe renal failure through attenuation of dNTP pools. Nat Genet 34:440–445.

Kinzler KW, Vogelstein B. 1996. Lessons from hereditary colorectal cancer. Cell 87:159–170.

Kohler SW, Provost GS, Fieck A, Kretz PL, Bullock WO, Sorge JA, Putman DL, Short JM. 1991. Spectra of spontaneous and mutagen-induced mutations in the lacI gene in transgenic mice. Proc Natl Acad Sci USA 88:7958–7962.

Komarov PG, Komarova EA, Kondratov RV, Christov-Tselkov K, Coon JS, Chernov MV, Gudkov AV. 1999. A chemical inhibitor of p53 that protects mice from the side effects of cancer therapy. Science 285:1733–1737.

Kuerbitz SJ, Plunkett BS, Walsh WV, Kastan MB. 1992. Wild-type p53 is a cell cycle checkpoint determinant following irradiation. Proc Natl Acad Sci USA 89:7491–7495.

Kusunoki Y, Kyoizumi S, Honma M, Kubo Y, Ohnishi H, Hayashi T, Seyama T. 2000. NK-mediated elimination of mutant lymphocytes that have lost expression of MHC class I molecules. J Immunol 165:3555–3563.

Lane DP. 1992. Cancer. p53, guardian of the genome. Nature 358:15–16.

Lasko D, Cavenee W, Nordenskjold M. 1991. Loss of constitutional heterozygosity in human cancer. Annu Rev Genet 25:281–314.

Lengauer C, Kinzler KW, Vogelstein B. 1998. Genetic instabilities in human cancers. Nature 396:643–649.

Levine AJ, Perry ME, Chang A, Silver A, Dittmer D, Wu M, Welsh D. 1994. The 1993 Walter Hubert lecture: the role of the p53 tumour-suppressor gene in tumorigenesis. Br J Cancer 69:409–416.

Li CY, Yandell DW, Little JB. 1992. Molecular mechanisms of spontaneous and induced loss of heterozygosity in human cells in vitro. Somat Cell Mol Genet 18:77–87.

Liang L, Shao C, Deng L, Mendonca MS, Stambrook PJ, Tischfield JA. 2002. Radiation-induced genetic instability in vivo depends on p53 status. Mutat Res 502:69–80.

Liber HL, Thilly WG. 1982. Mutation assay at the thymidine kinase locus in diploid human lymphoblasts. Mutat Res 94:467–485.

Liber HL, Call KM, Little JB. 1987. Molecular and biochemical analyses of spontaneous and X-ray-induced mutants in human lymphoblastoid cells. Mutat Res 178:143–153.

Liber HL, Yandell DW, Little JB. 1989. A comparison of mutation induction at the *tk* and *hprt* loci in human lymphoblastoid cells: quantitative differences are due to an additional class of mutations at the autosomal *tk* locus. Mutat Res 216:9–17.

Little JB, Nagasawa H, Keng PC, Yu Y, Li CY. 1995. Absence of radiation-induced G1 arrest in two closely related human lymphoblast cell lines that differ in p53 status. J Biol Chem 270:11033–11036.

Liu G, Parant JM, Lang G, Chau P, Chavez-Reyes A, El Naggar AK, Multani A, Chang S, Lozano G. 2004. Chromosome stability, in the absence of apoptosis, is critical for suppression of tumorigenesis in Trp53 mutant mice. Nat Genet 36:63–68.

Livingstone LR, White A, Sprouse J, Livanos E, Jacks T, Tlsty TD. 1992. Altered cell cycle arrest and gene amplification potential accompany loss of wild-type p53. Cell 70:923–935.

Loeb LA. 1991. Mutator phenotype may be required for multistage carcinogenesis. Cancer Res 51:3075–3079.

Lu X, Lane DP. 1993. Differential induction of transcriptionally active p53 following UV or ionizing radiation: defects in chromosome instability syndromes? Cell 75:765–778.

Mathonnet G, Leger C, Desnoyers J, Drouin R, Therrien JP, Drobetsky EA. 2003. UV wavelength-dependent regulation of transcription-coupled nucleotide excision repair in p53-deficient human cells. Proc Natl Acad Sci USA 100:7219–7224.

Mekeel KL, Tang W, Kachnic LA, Luo CM, DeFrank JS, Powell SN. 1997. Inactivation of p53 results in high rates of homologous recombination. Oncogene 14:1847–1857.

Morris SM, Manjanatha MG, Shelton SD, Domon OE, McGarrity LJ, Casciano DA. 1996. A mutation in the p53 tumor suppressor gene of AHH-1 $tk^{+/-}$ human lymphoblastoid cells. Mutat Res 356:129–134.

Morris SM. 2002. A role for p53 in the frequency and mechanism of mutation. Mutat Res 511:45–62.

Neuhausen SL, Marshall CJ. 1994. Loss of heterozygosity in familial tumors from three BRCA1-linked kindreds. Cancer Res 54:6069–6072.

Neuhof D, Ruess A, Wenz F, Weber KJ. 2001. Induction of telomerase activity by irradiation in human lymphoblasts. Radiat Res 155:693–697.

Nishino H, Knoll A, Buettner VL, Frisk CS, Maruta Y, Haavik J, Sommer SS. 1995. p53 wild-type and p53 nullizygous Big Blue transgenic mice have similar frequencies and patterns of observed mutation in liver, spleen and brain. Oncogene 11:263–270.

Olivier M, Eeles R, Hollstein M, Khan MA, Harris CC, Hainaut P. 2002. The IARC TP53 database: new online mutation analysis and recommendations to users. Hum Mutat 19:607–614.

Peng Y, Zhang Q, Nagasawa H, Okayasu R, Liber HL, Bedford JS. 2002. Silencing expression of the catalytic subunit of DNA-dependent protein kinase by small interfering RNA sensitizes human cells for radiation-induced chromosome damage, cell killing, and mutation. Cancer Res 62:6400–6404.

Pipiras E, Coquelle A, Bieth A, Debatisse M. 1998. Interstitial deletions and intrachromosomal amplification initiated from a double-